Petroleum Science 23 (2026) 365–382

Contents lists available at ScienceDirect

Petroleum Science

journal homepage: www.keaipublishing.com/en/journals/petroleum-science

Original Paper

Performance of steam injection process in layered heavy oil reservoirs: An experimental and numerical investigation

Xiu-Chao Jiang, Xiao-Hu Dong *, Hao Zhang, Tian-Yang Yin, Hui-Qing Liu

State Key Laboratory of Petroleum Resources and Engineering, China University of Petroleum (Beijing), Beijing, 102249, China

ARTICLE INFO

Article history:
Received 29 May 2025
Received in revised form
24 September 2025
Accepted 27 September 2025
Available online 1 October 2025

Edited by Yan-Hua Sun

Keywords:
Layered heavy oil reservoirs
Cyclic steam stimulation
Steam flooding
Scaled 2D model
Heated chamber
Production performance

ABSTRACT

Layered heavy oil reservoirs are widely distributed hydrocarbon resources and play a crucial role in fulfilling the global increasing demand for energy. Due to the existence of interlayer heterogeneity, however, the traditional commingled steam injection process has been confronted with the challenges of uneven production and poor performance in the field. In this study, to investigate the improvement effects of a separate steam injection process for the layered heavy oil reservoirs, combining the methods of experiments and numerical simulation, the expansion behavior of the heated chamber and production performance of these two steam injection modes (base case and improved case) are compared and analyzed. First, based on the 2D scaling criteria of steam stimulation experiments and actual properties of a typical layered heavy oil reservoir in China, the experimental parameters are obtained. During experiments, to better simulate the field operation condition, a 2D HTHP (high temperature and high pressure) thermal recovery experimental apparatus equipped with a pressure chamber is proposed. From the experimental observations, the advantages of the separate steam injection mode are illustrated from the expansion behavior of the heated chamber and the production performance characteristics. Thereafter, through a history matching of the experimental results, the laboratory-scale numerical simulation model is developed. Then, from the same-scale numerical simulation model, the steam flooding stage of the base case for the layered heavy oil reservoirs is divided into three phases, and the primary features and critical indices of different phases are obtained. Finally, the effects of reservoir properties and operation parameters on production performance and interlayer divergence are discussed. Experimental results show that the separate steam injection mode achieves uniform heated chamber expansion across layers, and the average proportion of heated chamber is 18% higher than that of the commingled steam injection process. Meanwhile, the improved case increases the final oil recovery factor by around 6%. The simulation results of the developed laboratory-scale numerical simulation model are in good agreement with the experimental observations. For the layered reservoirs with an interlayer permeability contrast of the oil layer reaching 3, it is recommended to adopt the separate steam injection mode. In addition, the optimum cyclic steam injection volume for the reservoir is 6000–7000 m^3, and the steam injection rate should be no more than 250 m^3/d. This paper contributes to a systematic understanding of steam stimulation performance with different steam injection modes for layered heavy oil reservoirs.

1. Introduction

The steam stimulation recovery process is a widely applied and primarily recommended approach in the development of heavy oil reservoirs, typically involving cyclic steam stimulation (CSS), steam flooding (SF), and steam-assisted gravity drainage (SAGD) (Dong et al., 2024; Li et al., 2023b; Sun et al., 2023b). Injecting steam into the reservoir can increase the temperature of the

* Corresponding author.
E-mail address: dongxh@cup.edu.cn (X.-H. Dong).

Peer review under the responsibility of China University of Petroleum (Beijing).

https://doi.org/10.1016/j.petsci.2025.09.041

reservoir, reduce the oil viscosity, and improve the oil mobility. Steam stimulation technology has been successfully performed in various fields, such as Lake Maracaibo in Venezuela, Cold Lake in Canada, and Liaohe Oilfield in China (Dong et al., 2019; Yan et al., 2025). Generally, it is an essential prerequisite for requiring a high oil–steam ratio (OSR) to ensure the operation of the steam stimulation process (Yan et al., 2025). However, most of the steam stimulation recovery processes in the field have entered into an exhaustion stage, facing the problems of steam breakthrough and low sweep efficiency (Dong et al., 2019, 2022; Sun et al., 2022). Especially for layered heavy oil reservoirs, due to the existence of significant heterogeneity in reservoir properties, these problems are more prominent in a later stage of the steam stimulation process (Gao et al., 2020; Wu et al., 2018). As the climate and environment continue to worsen worldwide, the green, economical, and sustainable exploitation of hydrocarbon resources has become the top concern for global oil and gas enterprises (Pu et al., 2025; Rui et al., 2025; Sheng et al., 2025; Wang et al., 2022). Meanwhile, it is well known that the thermal recovery processes based on the injection of steam are still extensively applied in heavy oil reservoirs despite the high carbon emissions involved (Chai et al., 2024; Guan et al., 2023; Yan et al., 2025). Therefore, it is of great significance to find ways to produce heavy oil in a low-carbon and economic approach while ensuring the energy demands (Chai et al., 2024; Liu and Dong, 2022; Pratama and Babadagli, 2024; Zhu et al., 2022). Researchers have proposed the hybrid thermal recovery processes, i.e., additives-assisted steam stimulation, to improve the recovery performance of post-steamed heavy oil reservoirs (Liu and Dong, 2022; Lu et al., 2024; Pérez et al., 2022). Typically, the hybrid thermal recovery processes include the thermal-NCG (non-condensable gas) process (Austin-Adigio and Gates, 2019; Jamshid-nezhad, 2022; Jiang et al., 2024; Wang et al., 2023), thermal-chemical process (Hong et al., 2025; Liu et al., 2023; Wang et al., 2020), and thermal-solvent process (Huang et al., 2019; Li et al., 2023a; Yang et al., 2024b; Venkat Venkatramani and Okuno, 2017). Extensive experimental investigations illustrate that the recovery mechanisms of additives primarily include the supplement reservoir energy, heat insulation, thief zone plugging, conformance control, and assisted viscosity reduction (Dang et al., 2025; Dong et al., 2019; Pang et al., 2024; Zhu et al., 2024). In addition, the electrical heating-assisted steam stimulation recovery process provides a promising solution for low-carbon, economical, and sustainable development in heavy oil reservoirs (He et al., 2024; Li et al., 2025b; Yan et al., 2025; Yang et al., 2024a).

Due to the constraints of operation costs and injection techniques, the commingled injection process is commonly adopted in the field to recover heterogeneous reservoirs (Kang et al., 2021; Peng et al., 2025; Wang et al., 2024). Many studies of recovery characteristics of stratified reservoirs with water flooding are reported, and the adopted methods primarily include experimental simulation (Chen et al., 2024; Huang et al., 2015; Wang et al., 2021; Zhao et al., 2023), theoretical modelling (Peng et al., 2025; Shen et al., 2022; Wang et al., 2024), and numerical simulation (Ding et al., 2022; Song et al., 2024; Tang et al., 2022). Through multi-tube water flooding experiments, Huang et al. (2015) quantitatively evaluated the interlayer interference in multilayer commingled production for ordinary heavy oil reservoirs, and obtained the empirical expressions of the interference coefficient for fluid and oil production indices. Based on experimental results of a heterogeneous reservoir model with a partly connected barrier, Zhao et al. (2023) established a numerical inversion model and investigated the evolution law of dominant flow channels in the water flooding process. They compared the water control performance of different regulation measures during the high water-cut period. To address the intensified reservoir heterogeneity after water flooding, Chen et al. (2024) studied the profile control capability of AOS-DYG (a polymer-enhanced foam) through parallel cores with different permeability contrasts. Using a heterogeneous microscopic model, Wang et al. (2021) conducted oil displacement experiments with polymer solutions, and they argued that under certain sweep conditions, improving oil displacement efficiency should be the focus for the heterogeneous heavy oil reservoirs. With the effects of the formation inclination, reservoir heterogeneity, and gravity on the two-phase flow process considered, Peng et al. (2025) extended the application scopes of the Buckley–Leverett equation. Their model could predict the position of the displacement front under different heterogeneity conditions. Wang et al. (2024) proposed an improved Lorenz method with the reservoir engineering theory, and validated the method by physical simulation experiments and production data from the block KL-A and KL-B in Bohai, China. Their results showed a significant enhancement in the relevance between the Lorenz coefficient and oil recovery factor. According to the production performance, Shen et al. (2022) established an evaluation framework for identifying high-water-consumption layers in stratified heterogeneous reservoirs and verified its effectiveness with field results. Based on the simulation results of reservoir numerical simulation software, Tang et al. (2022) analyzed the distributions of the streamline and oil saturation for the water flooding process in a multilayer reservoir. Aiming at addressing the issue of poor performance with the water flooding process for carbonate reservoirs in the Middle East, Song et al. (2024) proposed the separate-layer balanced water flooding development technology, and compared the production performances of different water injection modes. The results showed that with the conventional stratigraphic framework, under the same oil recovery factor conditions, the water cut of the R oilfield decreased by nearly 50% compared to that of the commingled water injection process. Based on an optimized emulsion flow model, Ding et al. (2022) developed a numerical simulator to describe the emulsion-assisted EOR process in heterogeneous porous media, and the simulated results could achieve good agreement with the experimental data. These studies confirmed that the permeability heterogeneity is a crucial factor impeding the uniform recovery across layers, and to some extent, revealed the necessity of adopting the layered injection process for stratified reservoirs.

Currently, the investigations on steam stimulation recovery process for stratified heavy oil reservoirs have focused on the aspects of field application (Gong et al., 2007; Liu, 2022; Ren et al., 2012; Zhao, 2009) and technology development (Cai and Zou, 2024; Dong, 2018; Liu et al., 2007), but few experimental studies were reported (Gao et al., 2020; Li et al., 2025a). In China, many field operations of steam stimulation have been implemented in the representative layered heavy oil reservoirs, including Qi40 and Jin45 in Liaohe Oilfield, Zhongerbei in Shengli Oilfield, and Jinglou in Henan Oilfield. However, influenced by interlayer heterogeneity, the steam stimulation recovery process in stratified heavy oil reservoirs frequently encounters problems such as uneven sweep efficiency among layers and severe steam channeling (Li et al., 2019; Liu, 2013; Shen et al., 2015; Wang, 2021; Zhao et al., 2022). For the issues of steam channeling and low oil recovery in heterogeneous heavy oil reservoirs, Gao et al. (2020) performed a 3D physical simulation experiment to investigate the profile control performance of a gel. The experimental results showed that the sweep efficiency and oil recovery of the subsequent steam flooding process increased by approximately 32% and 14%, respectively, after the injection of gel into the high-permeability layer. Considering the reservoir heterogeneity, Li et al. (2025a) conducted the flue gas-assisted VH-SAGD (the vertical-horizontal well

hybrid SAGD) experiments, and they studied the enhancement mechanisms of flue gas in VH-SAGD and the effect of barrier length on the oil recovery. Most reported steam stimulation recovery processes for stratified heavy oil reservoirs are carried out with the commingled steam injection mode (Cai and Zou, 2024; Liu, 2022). The injected steam preferentially enters the high-permeability layer and recovers the heavy oil with the commingled steam injection process. On account of the significant viscosity contrast between the steam and heavy oil, the high-permeability layer absorbing more steam exhibits lower flow resistance (Gao et al., 2020; Liu et al., 2023; Wu et al., 2015). Meanwhile, the interlayer steam injection amount varies significantly with the commingled steam injection process; thus, the inherent reservoir heterogeneity is further intensified by the steam erosion (Liu and Dong, 2022; Sun et al., 2023a; Wu et al., 2018). Based on the discussion above, it can be found that the commingled steam injection process is confronted with the challenges of uneven production and poor performance. However, for stratified heavy oil reservoirs, the separate steam injection process can enhance the steam utilization efficiency and vertical sweep efficiency, and improve the oil recovery and oil–steam ratio (Cai and Zou, 2024; Hoyos Perdomo et al., 2014; Wang et al., 2017; Zhang et al., 2025). With the advances in separate steam injection technologies, the layered steam stimulation recovery process has been performed in some stratified heavy oil reservoirs in China, such as the Shan10 reservoir in the Shengli Oilfield and the Tan91 in the Jilin Oilfield (Sun, 2020; Xiong et al., 2016; Wang et al., 2018). In addition, the advantages of the improved injection process for reducing carbon emissions and enhancing oil recovery are widely recognized (Cai and Zou, 2024; Chai et al., 2024; Guan et al., 2023; Pratama and Babadagli, 2024). Although some literature has discussed the effect of heterogeneity on heavy oil reservoirs with steam stimulation process (Araújo et al., 2022; Gao et al., 2020; Li et al., 2025a), a systematic investigation on the performance of the steam stimulation recovery process for stratified heavy oil reservoirs is still lacking.

In this paper, the features of the commingled steam injection process and the separate steam injection process for layered heavy oil reservoirs are analyzed through two groups of physical experiments and a series of numerical simulation runs. In Section 2, the detailed design, procedures, and results of cyclic steam stimulation to steam flooding experiments are provided. Then, the same-scale numerical simulation models are developed through a history matching of the experimental observations in Section 3. Furthermore, based on the dimensionless injection/production performance curves of the base case, the steam flooding stage is divided into three phases: thermal communication phase, thermal displacement phase, and thermal breakthrough phase. Afterwards, the effects of reservoir properties and operation parameters on production performance and interlayer divergence are analyzed in detail. The main conclusions are provided in Section 4.

2. Experimental materials and methods

In this study, cyclic steam stimulation to steam flooding experiments are conducted in two modes of steam injection processes, including a commingled steam injection experiment and a separate steam injection experiment. The former can be considered the base case, and the latter is the improved counterpart.

2.1. Experimental materials

The oil sample used in this study is the wellhead dead oil from a typical layered heavy oil reservoir in China. The relationship between the oil viscosity and temperature is shown in Fig. 1, and the gas-free heavy oil viscosity at the initial reservoir temperature condition (40 °C) is 627 mPa·s. Deionized water is used to establish initial fluid saturation and generate steam. Quartz sand with 80–120 mesh is used to prepare the reservoir model.

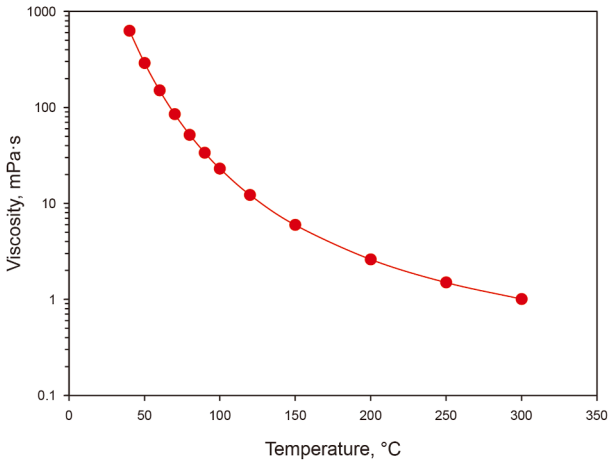

Fig. 1. The viscosity of heavy oil versus temperature.

2.2. Experimental apparatus

A 2D experimental assembly, which satisfies the requirements of cyclic steam stimulation to the steam flooding process, is utilized to conduct the physical simulation process, as illustrated in Fig. 2. As shown, the 2D model consisting of three reservoir submodels is used in this study to simulate the layered reservoir with the permeability distribution of inverse rhythmic layering. In the experiment, to closely approximate the reservoir conditions of pressure and temperature, the pressure chamber is filled with silicone fluid to provide the model with an external pressure accompanied by the confining pressure pump, as shown in Fig. 2 (a), and to simulate initial reservoir temperature with a heating rod. Furthermore, the backpressure regulator (BPR), accompanied by a backpressure pump, is used to maintain a high-pressure condition in the reservoir model and enable stepwise pressure reduction at the producer. The heater band is wrapped around the pipelines to compensate for the heat loss to the atmosphere. The 2D model (35 cm in length, 9 cm in width, and 30 cm in height) primarily consists of temperature-resistant epoxy resin, clay, oil sand, and wells. To prevent the steam breakthrough along the model surface, the inner surface is covered by a layer of earthenware clay, and its thickness is about 5 mm, as shown in Fig. 2(b). A set of thermocouples is used to monitor temperature variations within the reservoir model, and the data are collected through the data acquisition box and computer. The design of an oil layer (30 cm in length, 4 cm in width, and 5 cm in height) is shown in Fig. 2(b), and the wells are positioned on either side of the model with a well spacing of 27 cm. Once the 2D physical model is ready for the cyclic steam stimulation to steam flooding experiment, it will be moved into the pressure chamber.

The cyclic steam stimulation process is performed on both sides of the model with six huff and puff cycles. After the cyclic steam stimulation process, the well at the left end of model is served as the injector and the well at the right end of model is served as the producer by operating the control valves to conduct steam flooding process, as shown in Fig. 2. The thickness and permeability distribution of the oil layers in two experimental groups are identical, and the producers in different submodels are connected with a valve in both experiments. Compared with the separate

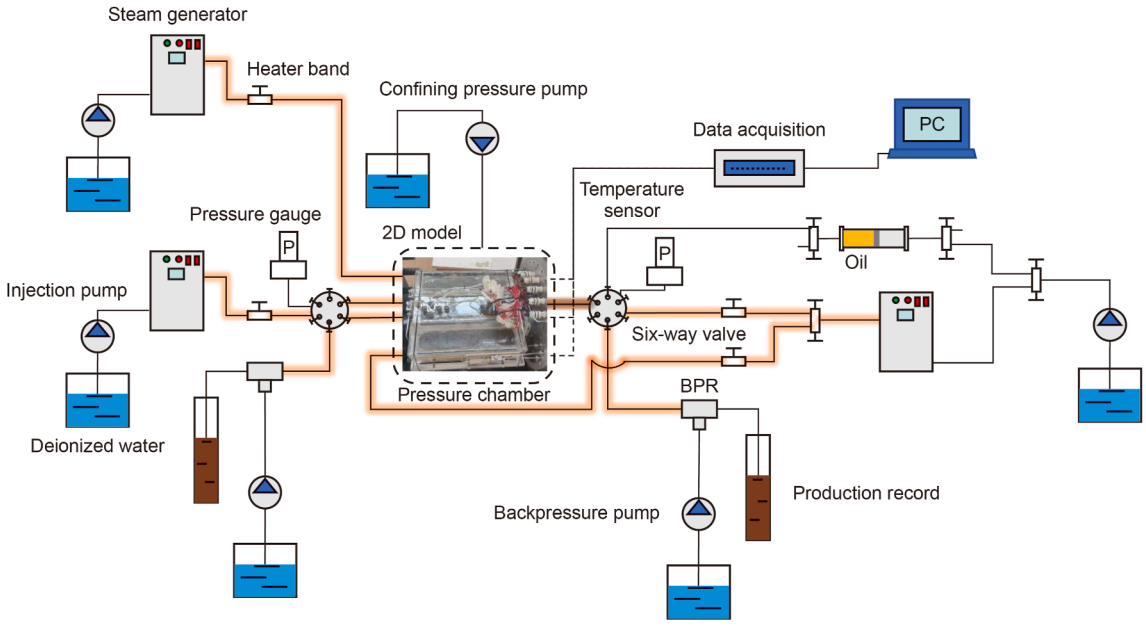

(a) General experimental assembly

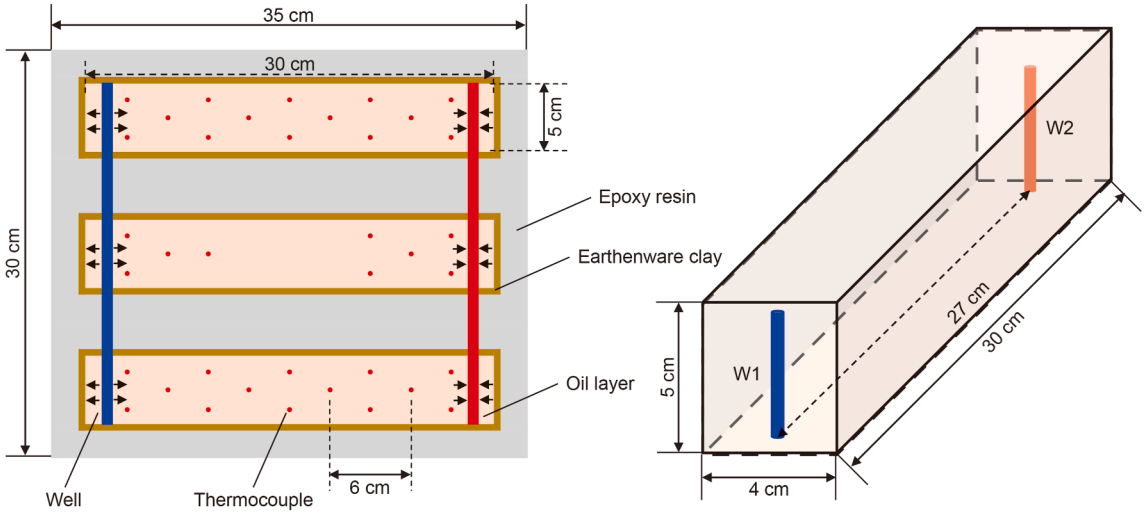

(b) Distribution of wells and thermocouples and 3D illustration of the reservoir model

Fig. 2. Schematic diagram of the 2D cyclic steam stimulation to steam flooding experiment.

steam injection experiment, during the steam flooding process, the steam is injected into the model with a valve connecting the injectors in three submodels for the commingled steam injection experiment. The total steam injection rate of the steam flooding process is set to 10 mL/min (cold water equivalent) for two experimental groups.

2.3. Experimental parameters

According to the reservoir properties of a typical layered heavy oil reservoir in China, the average permeability is 0.7 μm^2, and the total thickness and pay zone thickness are 60 and 36 m, respectively. Based on the reservoir properties, the initial reservoir pressure is 9 MPa, and the initial reservoir temperature is 40 °C. A physical model is developed based on the 2D scaling criteria of steam stimulation experiments, as shown in Table 1. Therefore, the experimental parameters of the model can be determined according to the scaling criteria, and the detailed experimental parameters are shown in Table 2.

In this study, the field-scale pay zone thickness, h_p, is 36 m, and that of the experimental model, h_m, is set as 15 cm. Thus, the geometric ratio applied in this experiment can be obtained. The well spacing in the experimental model can be calculated through Eq. (1). Therefore, the actual well spacing in our experiments can only represent one-third of the entire well spacing. Furthermore, the permeability of the experimental model is another critical parameter in the scaling process. The permeability of the physical model is usually above 100 μm^2 when the scaling criteria are strictly followed, resulting in the destruction of the law of kinetic similarity. Therefore, Forchheimer's law is applied to constrain the permeability in a laboratory-scale model (Dong et al., 2024).

$$r(L) = \frac{h_m}{h_p} = \frac{L_m}{L_p} \tag{1}$$

Table 1
2D scaling criteria of steam stimulation experiment.

Scaling criterion	Simulation parameter	Physical significance
$\frac{K\rho_o g t}{\phi \Delta S_o \mu_o L}$	Permeability	The ratio of gravity to vicious force
$\frac{\alpha t}{L^2}$	Production duration	The ratio of convection to thermal conduction
$\frac{Q_s}{N}$	Periodic injection volume	Dimensionless injection volume in CSS phase
$\frac{i_s t_s}{\phi \Delta S_o V}$	Steam injection rate	Dimensionless injection volume in SF phase

Table 2
Parameters of the field and physical simulation experiment.

Category	Parameter	Field	Experiment	Scaling ratio
Basic properties	Total thickness	60 m	25 cm	240
	Average permeability	0.7 μm^2	2.1 μm^2	–
	Pay zone thickness	36 m	15 cm	240
	Porosity	30%	30%	1
	Initial oil saturation	80%	80%	1
	Oil viscosity at reservoir conditions	627 mPa·s	627 mPa·s	1
	Initial reservoir temperature	40 °C	40 °C	1
	Initial reservoir pressure	9 MPa	9 MPa	1
	Steam temperature	300 °C	300 °C	1
CSS phase	Cold water equivalent per cycle	6000 m^3	30 mL	–
	Steam huff and puff cycles	6	6	1
SF phase	Production duration	1 a	9 min	240^2
	Steam injection rate	200 m^3/d	10 mL/min	–

2.4. Experimental procedure

(1) Model construction. The temperature-resistant epoxy resin is applied to prepare the shell of the layered reservoir model, and the size of the reservoir model is shown in Fig. 2.
(2) Quartz sand filling process. According to the test results of the permeability of quartz sand with different meshes (Dong et al., 2022), the quartz sand with the mesh of 80–100 and 100–120 is selected to simulate the layered heterogeneous reservoir. Specifically, quartz sand with 80–100 mesh is used for the high-permeability layer, quartz sand with 100–120 mesh is used for the low-permeability layer, and quartz sand with a mixing of 80–100 mesh and 100–120 mesh in a 1:1 ratio is used for the medium-permeability layer. Furthermore, it is assumed that the porosity of the reservoir model is about 30%; thus, the total volume of heavy oil and water can be calculated. Simultaneously, considering the initial oil saturation in Table 2, the ratio of oil volume and water volume is 4:1. Then, the quartz sand, heavy oil, and water are mixed to prepare the oil sand sample. During the oil sand filling process, the wells and thermocouples can be positioned in the designed locations, as shown in Fig. 2.
(3) Initial reservoir condition simulation. The oil sample and water are co-injected into the prepared model at a ratio of 4:1 to compensate for the reservoir void space formed in the oil sand filling process. Furthermore, to fully saturate the reservoir model, the injection ports will be changed once the previous ports reach a stable status. When the offset process for the initial saturation condition is completed, the model is placed into the pressure chamber. Simultaneously, the reservoir model is continuously heated until the temperature of the thermocouples reaches the initial reservoir temperature (40 °C). The oil sample and water are co-injected again into the model until the pressure of the model reaches the designed model pressure in Table 2.
(4) Steam stimulation process. The experiments are performed in two stages, including the cyclic steam stimulation process and the steam flooding process. During the stage of the cyclic steam stimulation process, the wells of both sides are simultaneously implementing the process of steam injection (15 min), soaking (2 min), and production (18 min). The approach of stepwise pressure reduction at the producer facilitates the subsequent steam flooding process. Specifically, from the first cycle to the fifth cycle, the pressure of BPR is gradually reduced from 9 to 5 MPa. After the fifth huff and puff cycle, the pressure of BPR is maintained at the previous pressure, i.e., the pressure for the steam flooding process (5 MPa). Then, the operation is switched to the stage of steam flooding. Well W1 serves as the injector, and Well W2 serves as the producer, as shown in Fig. 2. Once an obvious steam breakthrough is observed, the steam injection process is terminated.

2.5. Experimental results and discussion

The same experimental parameters are used in two groups of cyclic steam stimulation to steam flooding experiments, as shown in Table 2, and the volume of heavy oil sample saturated in either experimental model is about 540 mL, which provides a good basis to analyze the difference between the base case and improved counterpart.

2.5.1. Expansion behavior of the heated chamber

The temperature field for the cyclic steam stimulation to steam flooding process of the commingled steam injection mode is shown in Fig. 3. For the phase of cyclic steam stimulation, it is observed that the swept area of steam predominantly consists of the near vicinity of the huff and puff wells, as shown in Fig. 3(a) and (b), indicating limited recovery extent of cyclic steam stimulation process. Under the influence of steam overriding, the shape of the heated chamber at the end of the huff and puff process exhibits an inverted circular truncated cone. For the phase of steam flooding, the significant interlayer difference in expansion of the heated chamber can be observed. From Fig. 3(c) and (d), it is found that the interlayer difference gradually increases with continuous steam injection.

Fig. 4 shows the temperature field for the cyclic steam stimulation to the steam flooding process under a separate steam injection mode. As shown in Fig. 4(a) and (b), the shape of the heated chamber at the end of the huff and puff process also exhibits an inverted circular truncated cone. The temperature fields prior to the end of the steam flooding process are shown in Figs. 3(d) and 4(d). For the commingled steam injection process, it is observed that the heated chamber in the high-permeability layer is obviously larger than that of the medium-permeability layer and the low-permeability layer in Fig. 3(d), which means the injected steam preferentially flows through the high-permeability zone. Especially in a later stage of the steam flooding process, the effect of steam is dramatically reduced. Thus, an efficient steam injection mode is required. As a contrast, Fig. 4(c) and (d) illustrate that a uniform heated chamber expansion among different layers can be achieved by adopting a separate steam injection process. Obviously, the separate steam injection mode can improve the thermal efficiency of injected steam and benefit the thermal recovery process of heavy oil reservoirs with low carbon emissions.

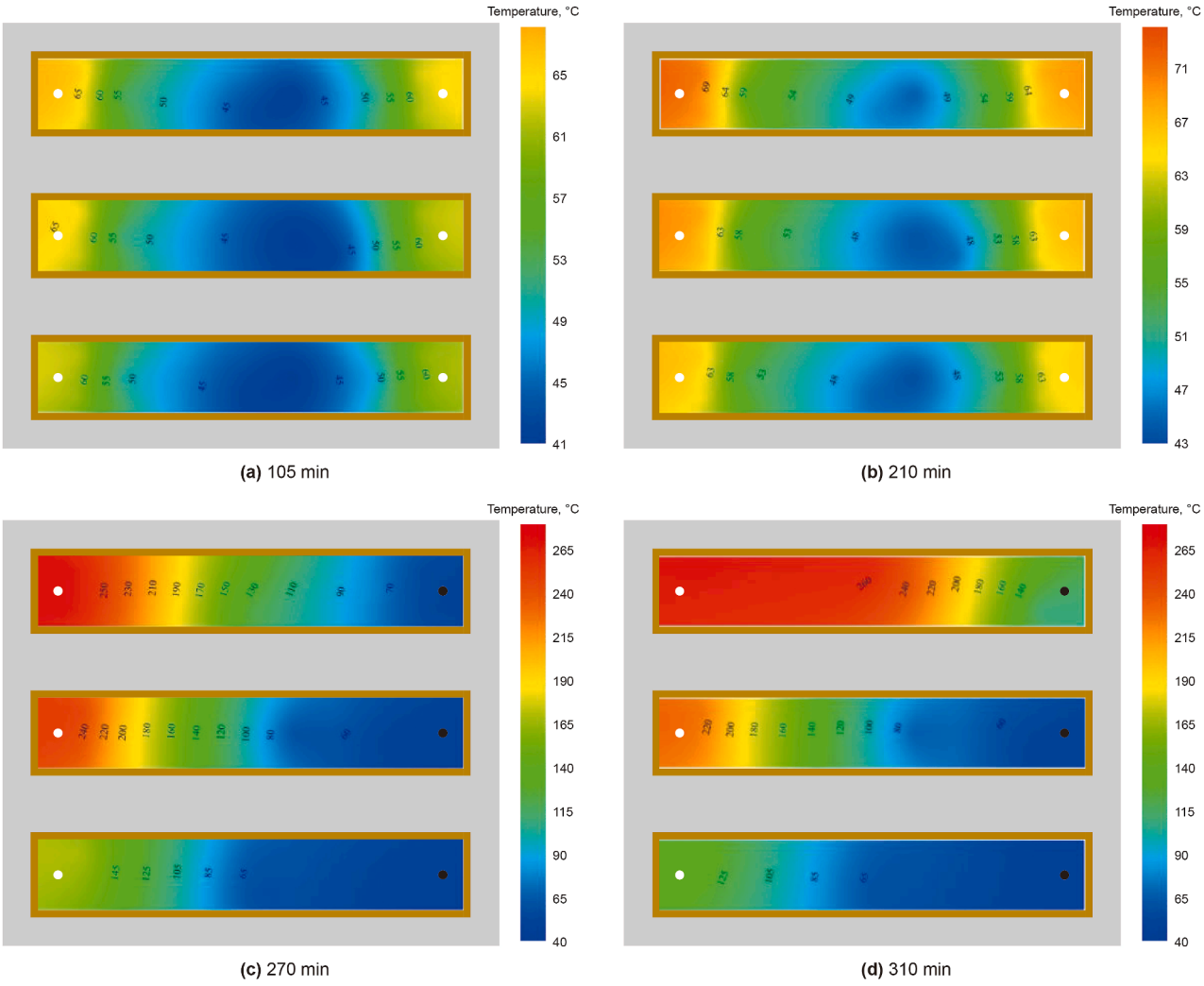

Fig. 3. Temperature fields of the commingled steam injection experiment.

From the temperature distributions at different phases, the differential expansion characteristics of heated chambers between these two steam injection methods are primarily observed during the steam flooding stage. This distinction arises because both methods employ the commingled steam injection method during the cyclic steam stimulation stage, while they utilize different injection schemes during the steam flooding stage. For the commingled steam injection experiment, steam tends to preferentially enter the high-permeability layer governed by the principle of minimal flow resistance, resulting in an uneven conformance. In contrast, the separate steam injection overcomes interlayer permeability contrasts by allocating steam volume to individual sublayers, achieving a uniform development of heated chambers in the layered heavy oil reservoirs.

Considering the viscosity of heavy oil and temperature conform to Arrhenius equation within the range of 30–90 °C, the temperature of the inflection point can be approximately determined by the temperature point at which the activation energy of heavy oil increases (Shan, 2023). According to the oil viscosities at different temperature conditions in Fig. 1, the temperature point is 60 °C where the activation energy of heavy oil increases. Simultaneously, the pressure for the steam flooding process is 5 MPa, corresponding to the saturated steam temperature of 263 °C. In order to quantitatively evaluate the expansion behavior of the heated chamber in the process of cyclic steam stimulation to steam flooding, based on the temperature field results, the proportions of the heated chamber (60 °C < T < 263 °C) and the steam chamber (T > 263 °C) can be obtained by the temperature of the inflection point and the saturated steam temperature.

Fig. 5 shows the results of the proportions of the heated chamber and the steam chamber. For the commingled steam injection experiment, it could be observed that the high-permeability layer (Layer 1) has a higher heated chamber proportion, which is attributed to the permeability distribution of inverse rhythmic layering. As shown in Fig. 5(a), the proportion of the heated chamber in the medium-permeability layer (Layer 2) and the low-permeability layer (Layer 3) begins to decrease approximately at 300 min, indicating that the steam channeling occurs in the high-permeability layer. Simultaneously, as it is switched to the steam flooding process, the temperature in the high-permeability layer gradually increases to the saturated steam temperature, initiating the development of a steam chamber, and the proportion of the steam chamber presents a characteristic sigmoidal ('S'-shaped) growth pattern.

As a contrast, from Fig. 5(b), it is observed that the proportion of the heated chamber among different layers for the separate steam injection experiment is obviously more uniform than that of the commingled steam injection case. Furthermore, the steam chamber occurs in all layers following the process of steam flooding, and the proportion of the steam chamber exhibits an analogous

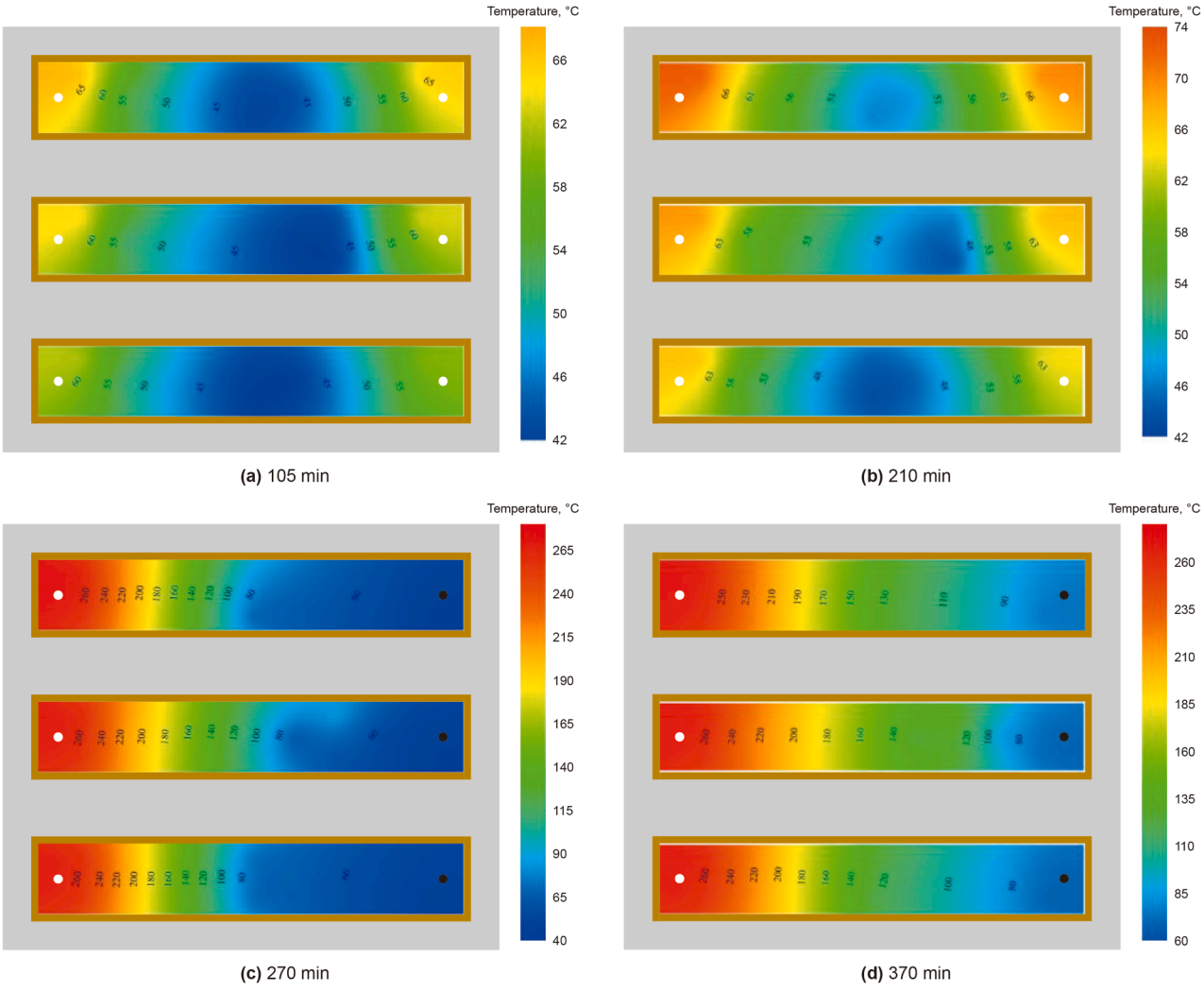

Fig. 4. Temperature fields of the separate steam injection experiment.

growth pattern. In summary, considering the permeability distribution feature, more steam is preferentially injected into the high-permeability layer with the commingled injection mode, increasing the expansion rate and expansion area of the heated chamber for the high-permeability layer. The layered injection mode, meanwhile, could achieve a uniform expansion area among all layers in the heterogeneous reservoir by controlling the injection profile. From the results in Fig. 5(c), it is illustrated that the average proportion of the heated chamber is 18% higher for the improved case than that of the base case at 350 min. However, due to steam channeling, the average proportion of the steam chamber for the base case is 2% higher than that of the improved case.

2.5.2. Production performance characteristics

The results of oil rate, oil recovery, and cumulative oil–steam ratio (COSR) for the experiments are shown in Fig. 6(a) and (b). During the cyclic steam stimulation stage, the primary characteristics of production performance of both experiments are characterized by markedly periodical variation in oil rate, relatively stable cumulative oil–steam ratio, and gradually increasing oil production. As shown, the maximum oil production rate is approximately 14.0 mL/min during the second or third cycle, with a relatively short production duration. The phenomenon is mainly attributed to the small-scale experimental model and rapid pressure depletion in the cyclic steam stimulation process. For the steam flooding stage, it is observed that the production performance of the two sets of experiments exhibits distinct differences. As shown in Fig. 6, the maximum oil production rates of the base case and improved case are, respectively, 4.6 and 3.1 mL/min. However, the final oil recovery factors for the base case and the improved case are 47.9% and 53.8%, respectively. This represents an improvement of approximately 6% achieved by using the separate steam injection mode.

According to the production performance comparison between these two groups of experiments, it could be concluded that the impact of interlayer heterogeneity on the recovery effect during the flooding process for different steam injection modes exhibits a phased feature. Based on the results of the temperature field in Fig. 3(c), for the base case, at the beginning of the steam flooding stage, a greater volume of steam preferentially flows into the high-permeability layer, leading to a higher initial oil rate but also a more rapid production decline. As the flooding process proceeds, steam channeling gradually occurs in the high-permeability layer (Fig. 3(d)), intensifying the inherent interlayer heterogeneity and restricting the mobilization of oil in the medium-permeability layer and the low-permeability layer. Simultaneously, combining the results in Figs. 5 and 6, in contrast to the base case, it is illustrated that the improved case demonstrates superior performance in heterogeneous reservoirs by adjusting the steam injection profile, thereby promoting uniform oil recovery from multi-layer

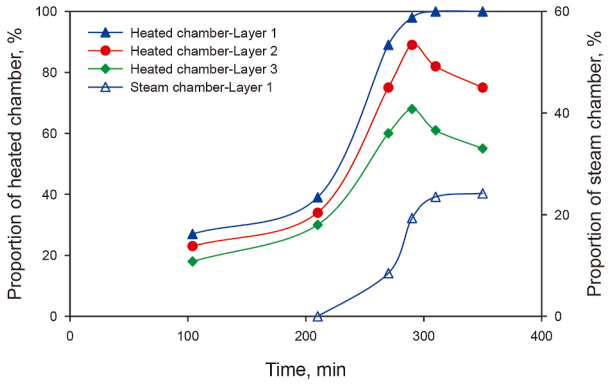

(a) Proportion of heated chamber/steam chamber for the commingled steam injection experiment

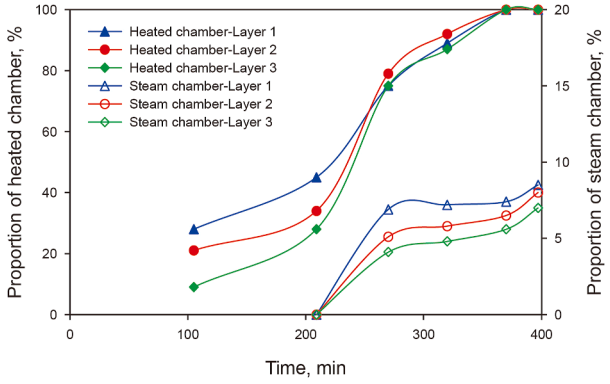

(b) Proportion of heated chamber/steam chamber for the separate steam injection experiment

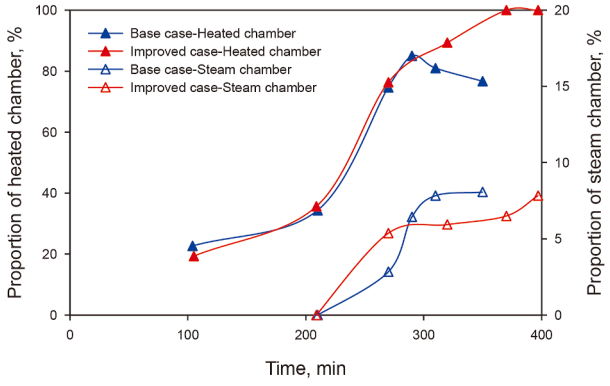

(c) Average proportion of heated chamber/steam chamber for different injection modes

Fig. 5. Proportion comparison of heated chamber/steam chamber for two groups of experiments.

heavy oil reservoirs. Both the expansion behavior of the heated chamber and the production performance characteristics provide conclusive evidence of the improvement effects of the separate steam injection process for the layered heavy oil reservoirs.

3. Laboratory-scale numerical simulation

3.1. Development of the model

Considering the prolonged duration and high complexity of physical simulation experiments, it is common to apply the

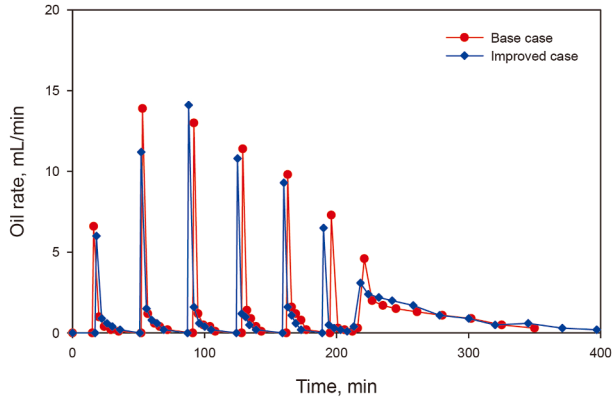

(a) Oil rate

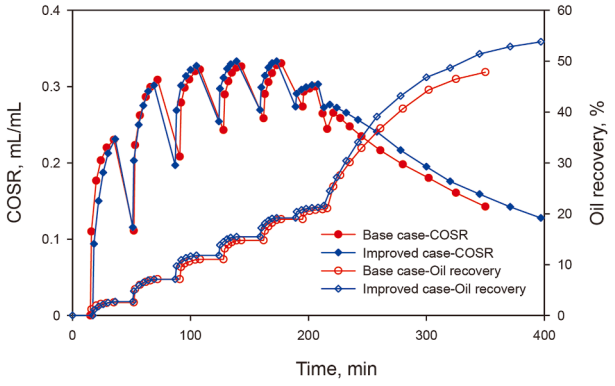

(b) Oil recovery factor and cumulative oil–steam ratio (COSR)

Fig. 6. Production performance comparison for two groups of experiments.

numerical simulation software to develop a laboratory-scale numerical simulation model. A numerical simulation model is developed using the same parameters as those in the experiment. Then, history matching of the experimental results is performed to calibrate the model so that it represents the actual layered reservoir.

A conceptual model is built in the CMG-STARS software, as shown in Fig. 7. The model uses a Cartesian grid with a size of $34 \times 8 \times 27$. The grid sizes of the oil reservoir, clay, and model surface are 1.0, 0.5, and 2.0 cm, respectively. The parameters of the numerical model, including the reservoir parameters and operation parameters, are based on the experimental data in Table 2.

3.2. History matching on the experimental result

Based on an established laboratory-scale numerical simulation model, the history matching of the experimental results can be achieved by adjusting the relative permeability and well index. The relative permeability applied in the history matching is shown in Fig. 8.

Fig. 9 shows the history matching results of the production performance between experimental data and numerical simulation results for the base case and improved case. It can be observed that the overall trends and primary characteristics are in good agreement for both experiments. For the oil recovery, the relative errors between experimental data and numerical simulation results for the base case and improved case are 5.4% and 5.9%, respectively, indicating the laboratory-scale model can effectively simulate the production performance of the physical model, and it

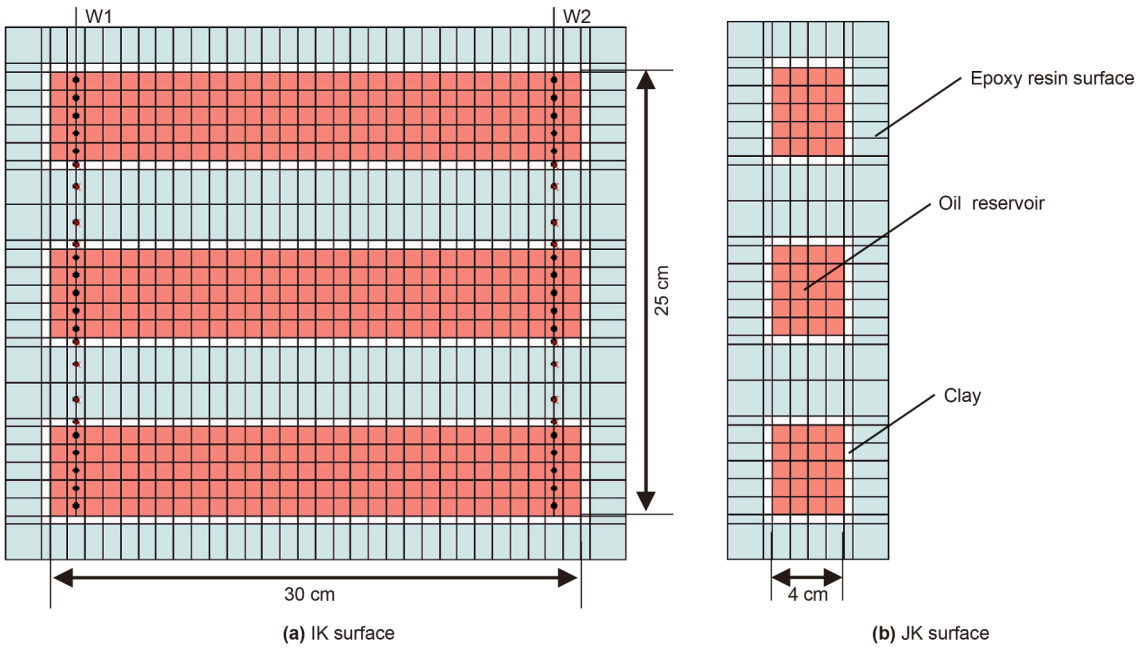

Fig. 7. Structural diagram of the laboratory-scale simulation model.

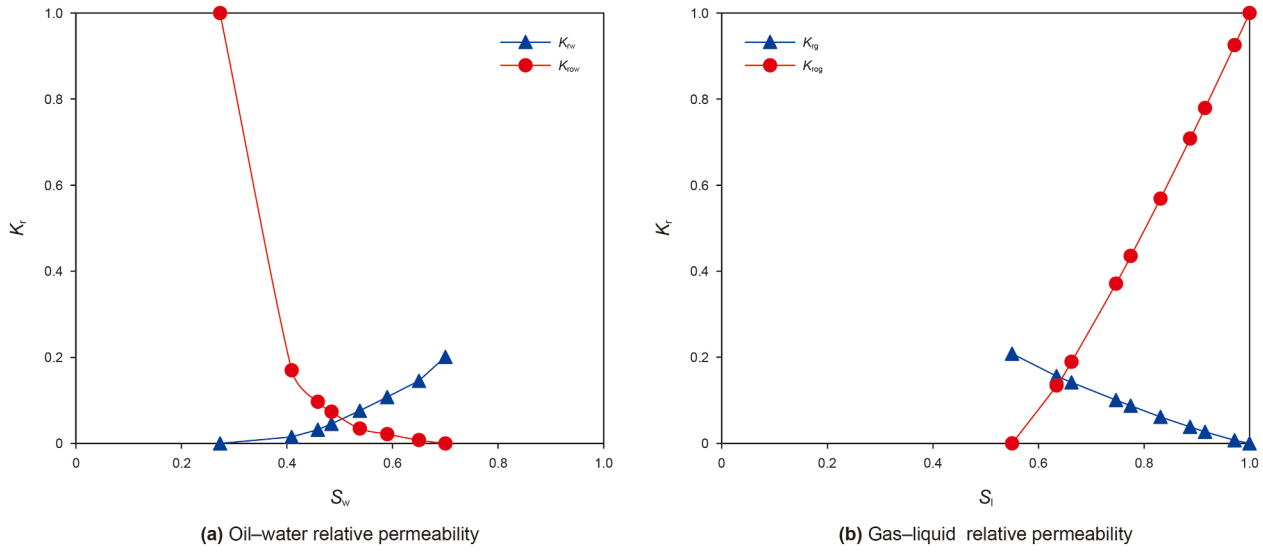

Fig. 8. Relative permeability curves in the model.

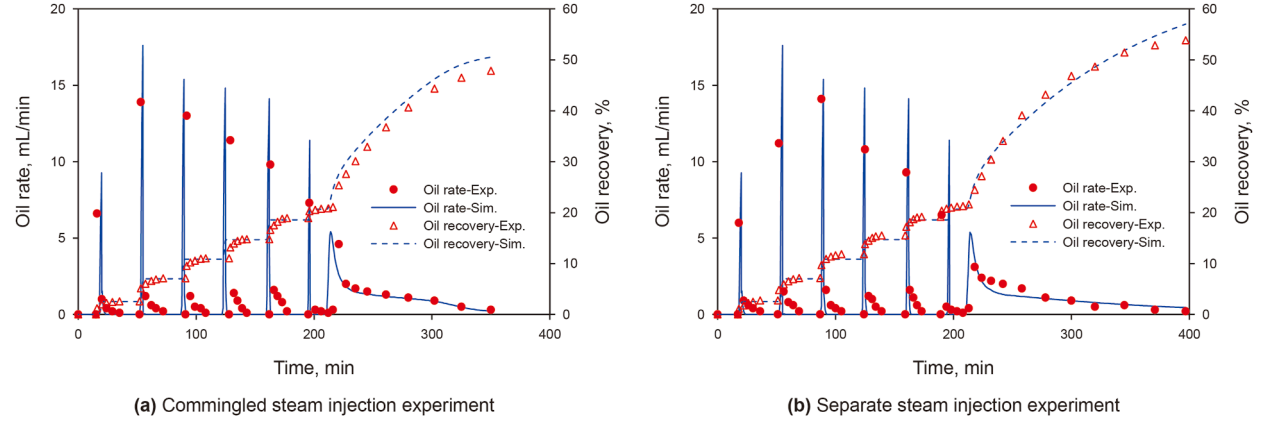

Fig. 9. Comparison of production performance between experimental data and simulated results.

could be used for the subsequent investigation and analysis of its production performance at different conditions.

The temperature fields of the cyclic steam stimulation (CSS) to steam flooding (SF) process for different steam injection modes are shown in Fig. 10. As shown, compared with the experimental temperature distributions in Figs. 3 and 4, a good agreement can be observed as well. Simultaneously, during the steam flooding process, it is found that the heated chamber of the improved case

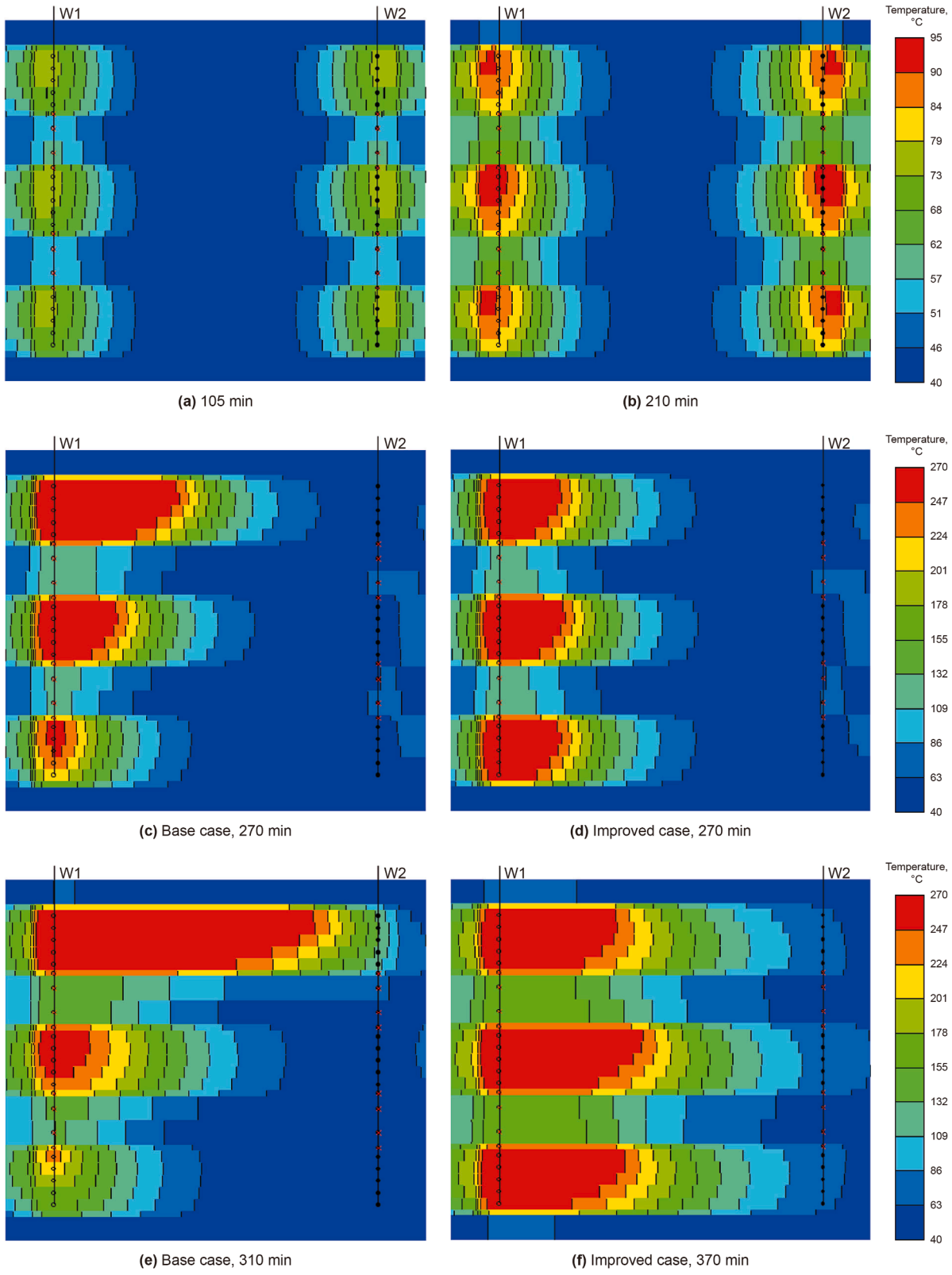

Fig. 10. Temperature fields of simulated results.

is larger; in addition, the steam overriding and steam breakthrough are effectively restrained. Therefore, for the improved case, it makes a more uniform expansion of the heated chamber in both intralayer zones and interlayer regions, leading to an enhanced sweep efficiency of injected steam in layered heavy oil reservoirs.

3.3. Stage division of the steam flooding process

Based on the established laboratory-scale numerical simulation model for the base case, the steam injection performance and oil production performance among different oil layers can be acquired. Then, the dimensionless steam injection ratio and dimensionless oil production ratio can be calculated through Eq. (2), and the dimensionless injection/production performance curves are shown in Fig. 11. Furthermore, according to the experimental observations and variations of the dimensionless injection/production performance curves, the steam flooding stage of the base case for the layered heavy oil reservoirs can be divided into three phases. Specifically, as shown in Fig. 11, these three phases include the thermal communication phase (I), the thermal displacement phase (II), and the thermal breakthrough phase (III).

$$q_{\mathrm{d}}^{i}=\frac{q_i}{\sum_{i=1}^{m} q_i} \tag{2}$$

The primary features of different phases are as follows: Firstly, the thermal communication phase spans from the initiation of the steam flooding process to a significant oil production increase in the thief zone, with marginal divergence in layer-wise steam injection profiles/oil production profiles. Secondly, for the thermal displacement phase, it is the primary production contribution stage, which accompanies increasing steam injection ratio and oil production ratio in the thief zone. Thirdly, during the thermal breakthrough phase, the steam channeling occurs in the thief zone; in addition, a low steam injection ratio, yet an increasing oil production ratio in the bypassed zones can be observed. Simultaneously, the critical indices of three phases for the steam flooding process, including the pore volume injected, stage recovery factor, and cumulative oil–steam ratio, are summarized in Table 3.

In order to further compare the typical differences of thermal communication phase (220 min), thermal displacement phase (275 min), and thermal breakthrough phase (325 min), based on the established laboratory-scale numerical simulation model, the distributions of temperature and oil saturation at different phases for the base case and improved case are obtained. The temperature distributions of different steam injection modes are shown in Fig. 12. It is observed that for the base case, the divergence in the behavior of the heated chamber across different oil layers progressively amplifies with continued flooding. Meanwhile, especially for the thermal displacement phase and the thermal breakthrough phase, the uniform interlayer expansion of the heated chamber for the improved case can be achieved. Fig. 13 shows the oil saturation distributions of different steam injection modes. Higher sweep efficiency and oil recovery can be observed for the improved case. Due to the existence of a thief zone, a large amount of remaining oil is still distributed in the medium-permeability layer and the low-permeability layer for the base case. This demonstrates that heterogeneity is an impeding factor in the conventional commingled steam injection process. These results could validate and supplement the experimental findings well.

3.4. Sensitivity analysis on production performance

Considering that the typical reservoirs are characterized by vertically stacked pay zones, significantly heterogeneous petrophysical properties, and laterally continuous barriers, in order to further investigate the effects of reservoir properties and operation parameters, based on the established laboratory-scale

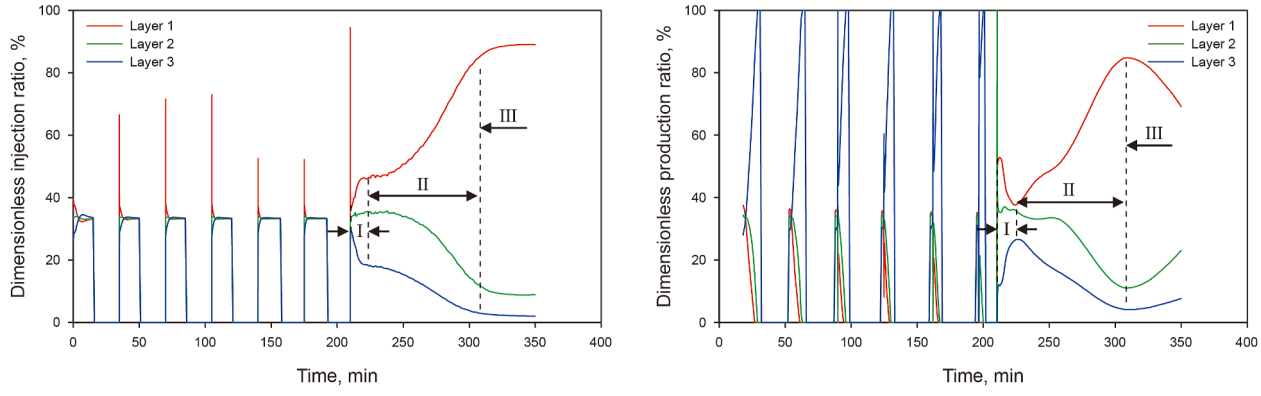

(a) Dimensionless steam injection ratio of different oil layers

(b) Dimensionless oil production ratio of different oil layers

Fig. 11. Curve of dimensionless injection/production performance for the layered reservoir.

Table 3
The critical indices of different steam flooding phases.

Stage	Index		
	Injection volume, PV	Stage recovery factor, %	Cumulative oil–steam ratio, mL/mL
Thermal communication phase	0–0.23	6.3	0.27–0.28
Thermal displacement phase	0.23–1.38	17.5	0.28–0.15
Thermal breakthrough phase	1.38–2.10	3.0	0.15–0.12

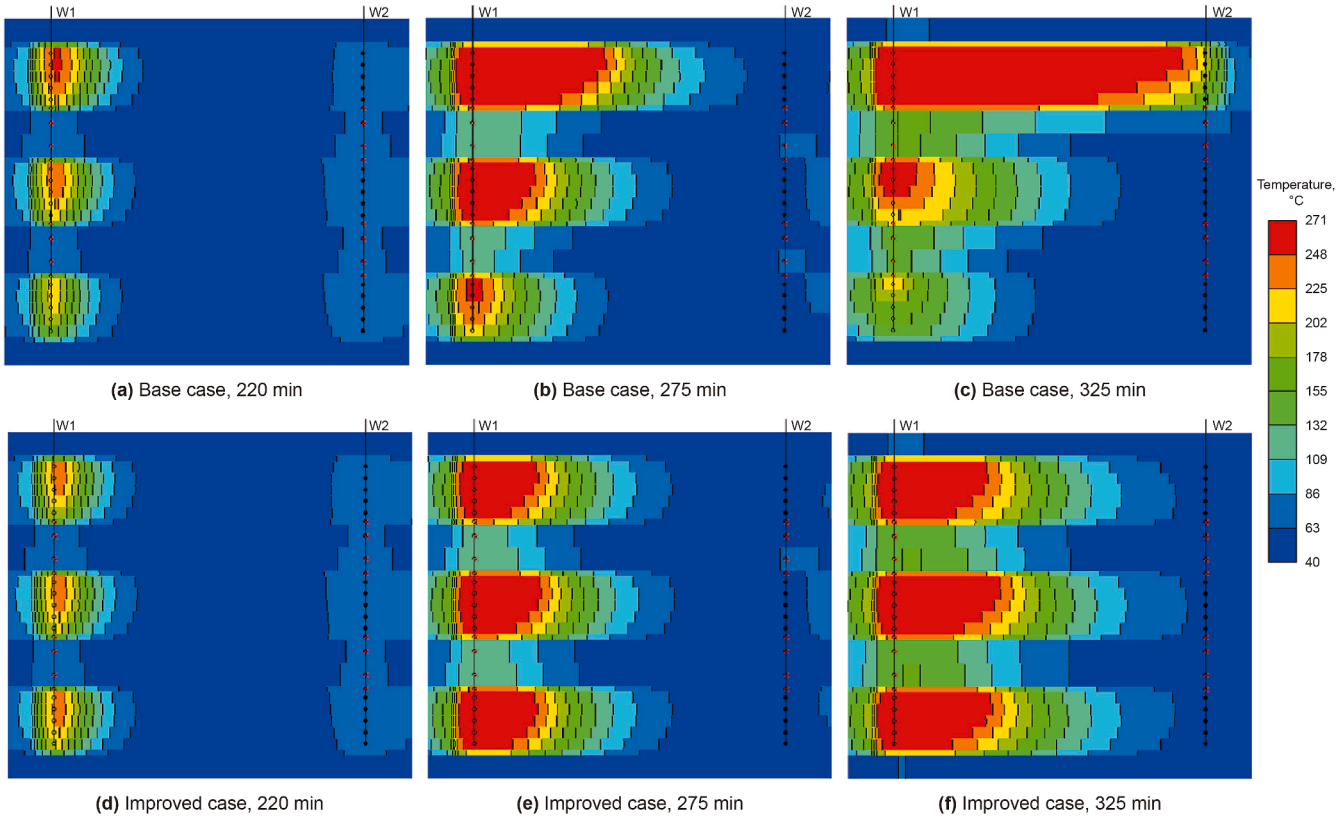

Fig. 12. Comparisons of temperature distributions at different phases.

numerical simulation model for the base case, a sensitivity analysis on production performance is conducted.

3.4.1. Reservoir properties

Firstly, the effects of different thickness ratios of oil layer to barrier (1, 2, 3, 4, and 5) on the oil recovery and cumulative oil–steam ratio are compared, as shown in Fig. 14(a). It is observed that with increasing thickness ratio of oil layer to barrier, the cumulative oil–steam ratio gradually improves, while the oil recovery exhibits a decline. For a large thickness ratio of oil layer to barrier, the heat lost in the barriers is less, thereby improving the heat utilization efficiency of injected steam. Meanwhile, although the original oil in place increases proportionally with the thickness ratio of the oil layer to the barrier, the extent to which oil recovery improves remains limited. Compared with the oil recovery of the case of 1 (the thickness of the oil layer equals that of the barrier), the oil recovery of the case of 3 at 350 min decreases by 3%. As the thickness ratio of the oil layer to the barrier falls below 3, the cumulative oil–steam ratio shows an obvious decline. Therefore, it is recommended to prioritize the thermal recovery process in reservoirs where the oil-layer-to-barrier thickness ratio is at least 3.

Next, the effects of different interlayer permeability contrasts of the oil layer (1, 2, 3, 4, and 5) on the oil recovery and cumulative oil–steam ratio are compared, as shown in Fig. 14(b). It is observed that as the interlayer permeability contrast of the oil layer increases, both the cumulative oil–steam ratio and oil recovery gradually decrease. Based on the experimental results in Fig. 3(d), it could be concluded that the existence of interlayer permeability heterogeneity impedes the recovery effect of oil in the medium-permeability layer and the low-permeability layer. Compared with the oil recovery of the case of 1 (homogeneous permeability distribution), the oil recovery of the case of 3 at 350 min decreases by 5%. The increasing interlayer permeability contrast of the oil layer further intensifies the interlayer heterogeneity of layered reservoirs, especially when it increases to 3; the cumulative oil–steam ratio drops below 0.15 mL/mL. Therefore, for the layered reservoirs with an interlayer permeability contrast of the oil layer reaching 3, it is recommended to adopt the separate steam injection mode to optimize the steam injection allocation among layers.

Furthermore, the effects of different interlayer thickness contrasts of the oil layer (1, 2, 3, 4, and 5) on the oil recovery and cumulative oil–steam ratio are compared, as shown in Fig. 14(c). It is observed that as the interlayer thickness contrast of the oil layer increases, both the cumulative oil–steam ratio and oil recovery gradually improve slightly. For a large interlayer thickness contrast of the oil layer, the oil recovery factor in the high-permeability layer improves, while that in the medium-permeability layer and the low-permeability layer decreases. Compared with the oil recovery of the case of 1 (homogeneous thickness distribution), the oil recovery of the case of 3 at 350 min improves by 1%. The determination of the thickness contrast threshold requires combining the interlayer divergence of layered reservoirs.

3.4.2. Operation parameters

Firstly, the effects of different steam injection volumes per cycle during the CSS phase (20, 25, 30, 35, and 40 mL) on the oil recovery and cumulative oil–steam ratio are compared, as shown in Fig. 15(a). It is observed that the effect of cyclic steam injection volume is more obvious in the CSS phase than in the SF phase. With increasing cyclic steam injection volume, the oil recovery gradually improves, while the cumulative oil–steam ratio exhibits a decline. As the cyclic steam injection volume varies from 20 to 40 mL, the incremental oil recovery at 210 min is about 4%, while

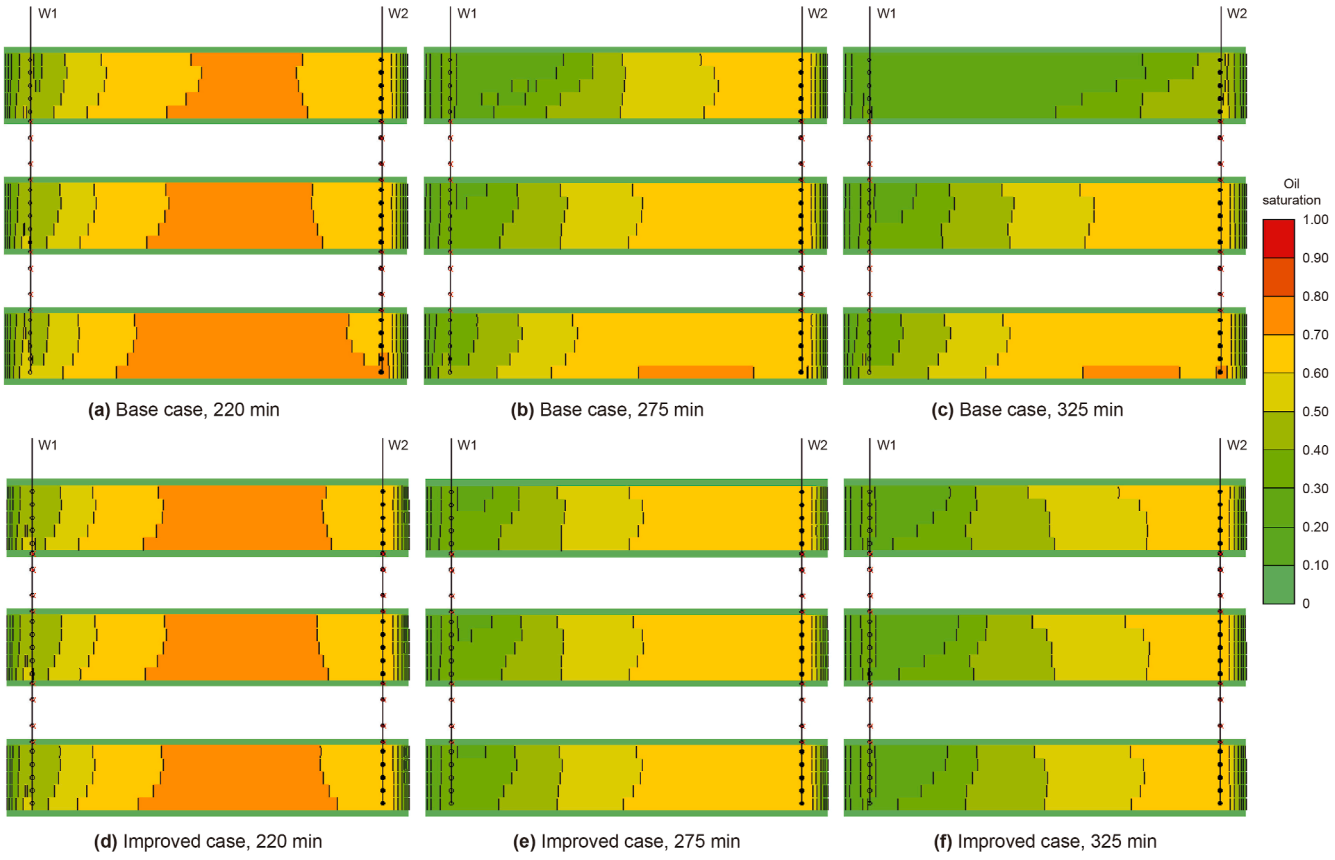

Fig. 13. Comparisons of oil saturation distributions at different phases.

that at 350 min is about 2%. According to the results of the oil recovery and cumulative oil–steam ratio, it is recommended to adopt a cyclic steam injection volume of no less than 30 mL. Based on the parameters in Table 2, the laboratory-scale volume of 30 mL corresponds to the field-scale 6000 m^3.

Next, the effects of different steam injection rates during the SF phase (5.0, 7.5, 10.0, 12.5, and 15.0 mL/min) on the oil recovery and cumulative oil–steam ratio are compared, as shown in Fig. 15(b). It is observed that as the steam injection rate increases, the cumulative oil–steam ratio gradually decreases, and an earlier maximum cumulative oil–steam ratio occurs. As the steam injection rate varies from 5.0 to 10.0 mL/min, the incremental oil recovery at 350 min is about 11%. However, once the steam injection rate exceeds 12.5 mL/min, an unexpected decline in oil recovery during the mid-late stage of steam flooding occurs. Therefore, it is recommended to adopt a steam injection rate of no more than 12.5 mL/min. Based on the parameters in Table 2, the laboratory-scale injection rate of 12.5 mL/min corresponds to the field-scale 250 m^3/d.

Furthermore, the effects of different steam qualities (0, 0.2, 0.4, 0.6, and 0.8) on the oil recovery and cumulative oil–steam ratio are compared, as shown in Fig. 15(c). It is observed that as steam quality increases, both the cumulative oil–steam ratio and oil recovery gradually improve. As the steam quality varies from 0 to 0.4, the incremental oil recovery at 350 min is about 6%. Once the steam quality exceeds 0.4, the improvement in the cumulative oil–steam ratio is slight. Simultaneously, low steam quality limits the development effects of the thermal recovery process. Therefore, the optimal steam quality is recommended to be around 0.4.

3.5. Sensitivity analysis on interlayer divergence

In this section, to quantitatively investigate the divergence among different oil layers, the concept of variation coefficient of heated chamber proportion is introduced, evaluating the heterogeneity of heated chamber expansion behavior for the layered heavy oil reservoirs, as shown in Eq. (3). Then, based on the established laboratory-scale numerical simulation model for the base case, the sensitivity analysis on interlayer divergence is conducted.

$$V_r = \sqrt{\frac{\sum_{i=1}^{m} (\alpha_i - \alpha_{avg})^2}{m\alpha_{avg}^2}} \tag{3}$$

3.5.1. Reservoir properties

Firstly, the effects of different thickness ratios of oil layer to barrier (1, 2, 3, 4, and 5) on the variation coefficient of heated chamber proportion are compared, as shown in Fig. 16(a). It is observed that with increasing thickness ratio of oil layer to barrier, the variation coefficient of heated chamber proportion gradually declines, and a later maximum variation coefficient occurs. Compared with the variation coefficient of the case of 1 (the thickness of oil layer equals that of the barrier), that of the case of 3 at 290 min drops from 0.30 to 0.22. As the thickness ratio of the oil layer to the barrier falls below 3, the variation coefficient of the heated chamber proportion shows an obvious rise, indicating the existence of significant heterogeneity of heated chamber expansion for the layered heavy oil reservoirs. Therefore, it is

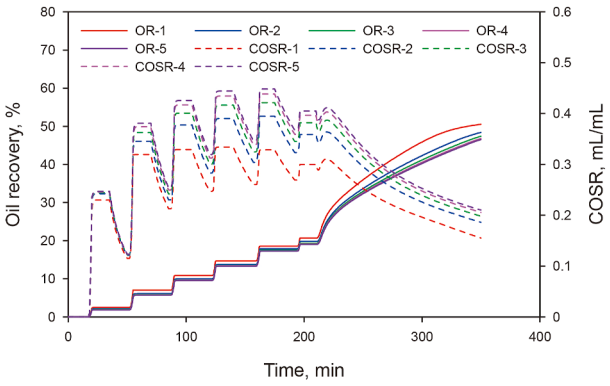

(a) Thickness ratio of oil layer to barrier

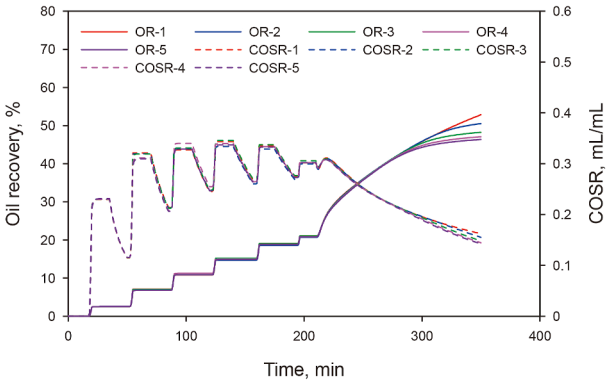

(b) Interlayer permeability contrast of the oil layer

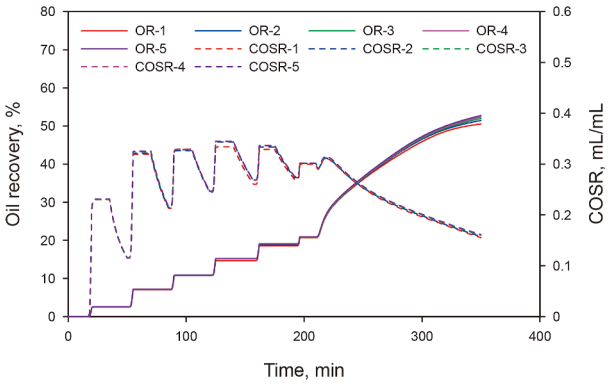

(c) Interlayer thickness contrast of the oil layer

Fig. 14. Effects of reservoir properties on production performance (OR: oil recovery).

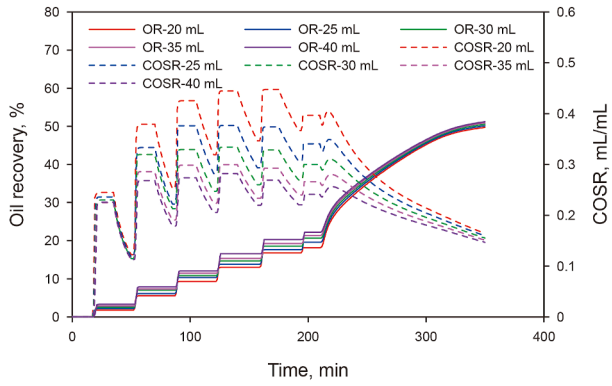

(a) Cyclic injection volume of steam during the CSS phase

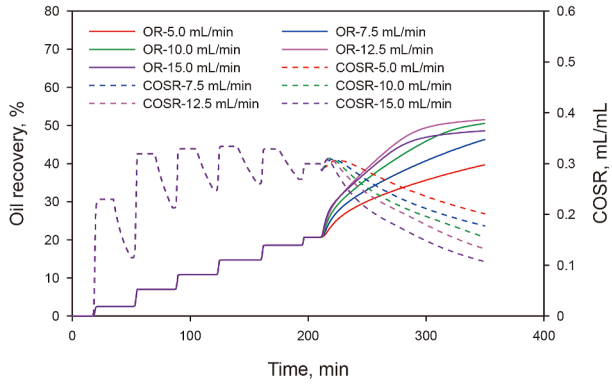

(b) Steam injection rate during the SF phase

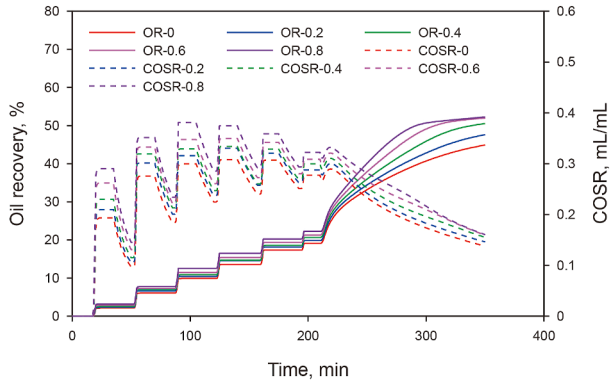

(c) Steam quality

Fig. 15. Effects of operation parameters on production performance.

recommended to prioritize the thermal recovery process in reservoirs with a thickness ratio of oil layer to barrier of no less than 3.

Next, the effects of different interlayer permeability contrasts of the oil layer (1, 2, 3, 4, and 5) on the variation coefficient of the heated chamber proportion are compared, as shown in Fig. 16(b). It is observed that as the interlayer permeability contrast of the oil layer increases, the variation coefficient of the heated chamber proportion gradually increases. Compared with the variation coefficient of the case of 1 (homogeneous permeability distribution), that of the case of 3 at 350 min increases from 0.04 to 0.39, illustrating that the interlayer heterogeneity of layered reservoirs has been further intensified by the large interlayer permeability contrast of the oil layer. Therefore, combining the effects of this permeability contrast on production performance, for the layered reservoirs with an interlayer permeability contrast of the oil layer reaching 3, it is recommended to adopt the separate steam injection mode to optimize the steam injection allocation among layers.

Furthermore, the effects of different interlayer thickness contrasts of the oil layer (1, 2, 3, 4, and 5) on the variation coefficient of the heated chamber proportion are compared, as shown in Fig. 16 (c). It is observed that as the interlayer thickness contrast of the oil layer increases, the variation coefficient of the heated chamber proportion gradually increases. Compared with the variation coefficient of the case of 1 (homogeneous thickness distribution), that of the case of 3 at 350 min increases from 0.29 to 0.46, indicating that the interlayer divergence is significantly intensified. Simultaneously, considering the variation threshold (0.30), for the layered reservoirs with an interlayer thickness contrast of the oil

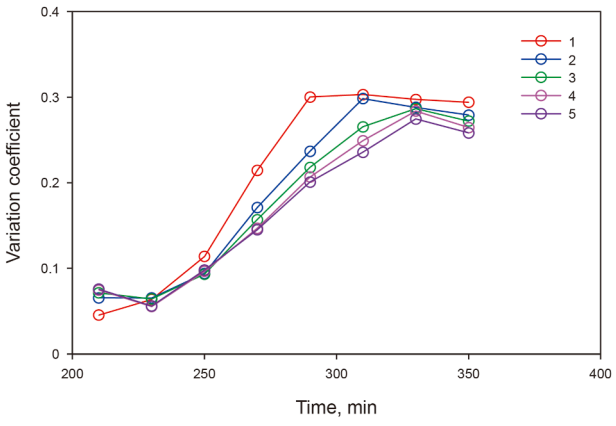

(a) Thickness ratio of oil layer to barrier

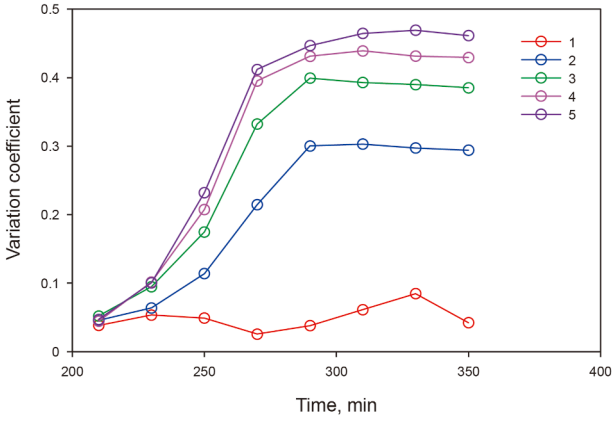

(b) Interlayer permeability contrast of the oil layer

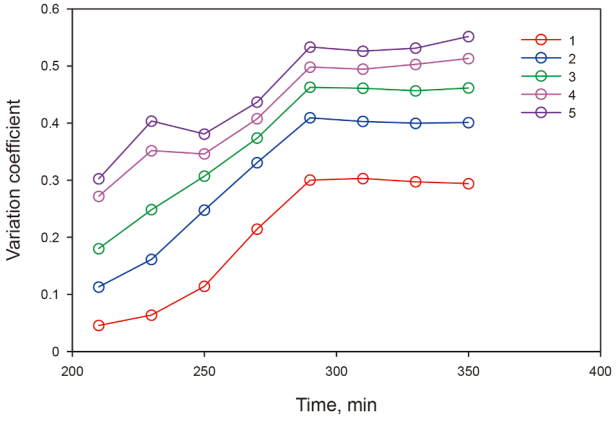

(c) Interlayer thickness contrast of the oil layer

Fig. 16. Effects of reservoir properties on interlayer divergence.

layer reaching 3, it is recommended to subdivide reservoir intervals into independent production units.

3.5.2. Operation parameters

Firstly, the effects of different steam injection volumes per cycle during the CSS phase (20, 25, 30, 35, and 40 mL) on the variation coefficient of heated chamber proportion are compared, as shown in Fig. 17(a). Generally, it is observed that with increasing cyclic steam injection volume, the variation coefficient of the heated chamber proportion gradually declines. As the cyclic steam injection volume varies from 20 to 35 mL, the variation coefficient at 350 min declines from 0.31 to 0.28. However, once the cyclic steam injection volume exceeds 35 mL, an unexpected increase in the variation coefficient during the late stage of steam flooding occurs. Therefore, combining the effects of cyclic steam injection volume on production performance, the optimal cyclic steam injection volume is recommended to be 30–35 mL. Based on the parameters in Table 2, the corresponding field-scale value is 6000–7000 m^3.

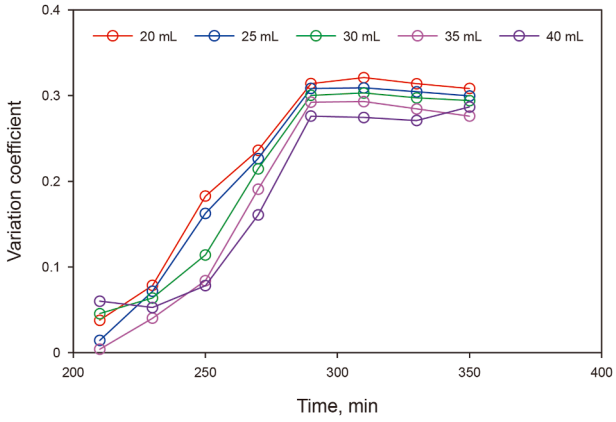

(a) Cyclic injection volume of steam during the CSS phase

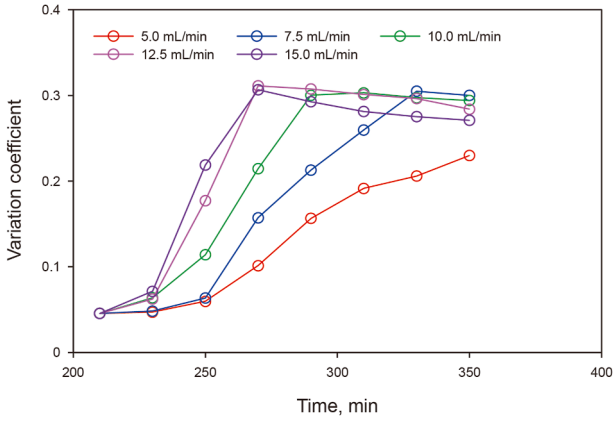

(b) Steam injection rate during the SF phase

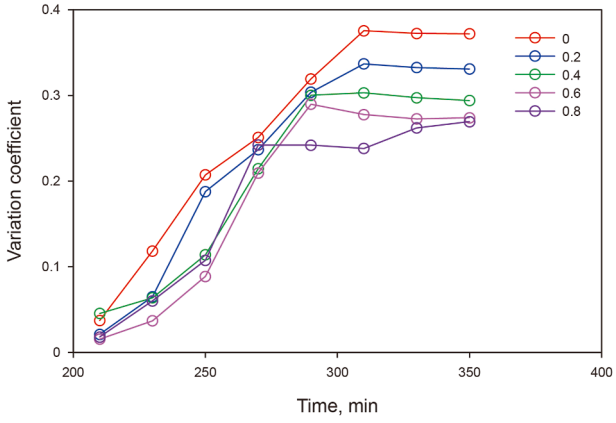

(c) Steam quality

Fig. 17. Effects of operation parameters on interlayer divergence.

Next, the effects of different steam injection rates during the SF phase (5.0, 7.5, 10.0, 12.5, and 15.0 mL/min) on the variation coefficient of heated chamber proportion are compared, as shown in Fig. 17(b). It is observed that all the cases possess the same value of maximum variation coefficient of heated chamber proportion, except the case of 5.0 mL/min. As the steam injection rate increases, an earlier maximum variation coefficient of heated chamber proportion occurs, indicating an earlier time of steam breakthrough. As the steam injection rate varies from 7.5 to 12.5 mL/min, the corresponding time of steam breakthrough varies approximately from 330 to 270 min. Therefore, combining the effects of steam injection rate on production performance, the optimal steam injection rate is recommended to be no more than 12.5 mL/min. Based on the parameters in Table 2, the corresponding field-scale value should be kept at most 250 m^3/d.

Furthermore, the effects of different steam qualities (0, 0.2, 0.4, 0.6, and 0.8) on the variation coefficient of heated chamber proportion are compared in Fig. 17(c). It is observed that, except for the case of 0.8, as the steam quality increases, the variation coefficient of the heated chamber proportion gradually declines. As the steam quality varies from 0 to 0.6, the variation coefficient at 350 min declines from 0.37 to 0.27. Therefore, combining the effects of steam quality on production performance, the optimal steam quality is recommended to be around 0.4.

4. Conclusions

In this paper, based on the scaling criteria of a 2D steam stimulation experiment, two groups of cyclic steam stimulation (CSS) to steam flooding (SF) experiments are conducted to investigate the effects of interlayer heterogeneity and separate steam injection mode. From the experimental results, the expansion behavior of the heated chamber and the production performance of different steam injection modes are analyzed in detail. Meanwhile, through the history matching of the experimental results, a laboratory-scale numerical simulation model is developed. Thereafter, some sensitivity analyses on production performance and interlayer divergence are performed. The main concluding remarks are drawn as follows.

(1) From the experimental results, it is found that the mode of separate steam injection can achieve a uniform heated chamber expansion for layered heavy oil reservoirs, and improve the average proportion of heated chamber by 18% more than that of the commingled steam injection process at 350 min. With the same steam injection rate, the final oil recovery factor of the separate steam injection can reach 53.8%, while that of the base case is 47.9%, resulting in an increment of around 6%.

(2) A laboratory-scale numerical simulation model with the same parameter settings is developed. By adjusting the relative permeability and well index, the overall trends and primary characteristics of production performance of simulation results are in good agreement with experimental data, and the relative errors of oil recovery between experimental data and numerical simulation results for the two cases are within 6%. Furthermore, a good agreement on heated chamber expansion can also be observed, indicating that the developed numerical model can represent the physical model.

(3) Based on the developed numerical model, the steam flooding process of the base case can be divided into three phases: thermal communication phase, thermal displacement phase, and thermal breakthrough phase. The primary features and critical indices of different phases are analyzed and summarized. Besides, the temperature fields and oil saturation fields at different phases for the base case and improved case are compared, illustrating that higher sweep efficiency and oil recovery can be obtained for the improved case.

(4) The effects of the thickness ratio of the oil layer to the barrier and the interlayer permeability contrast of the oil layer on oil recovery and cumulative oil–steam ratio are remarkable, and a large cyclic steam injection volume and a small steam injection rate benefit the uniform recovery across layers. Combining the results of production performance and interlayer divergence, for the layered reservoirs with an interlayer permeability contrast of the oil layer reaching 3, it is recommended to adopt the separate steam injection mode. In addition, the optimum cyclic steam injection volume for the reservoir is 6000–7000 m^3, and the steam injection rate should be no more than 250 m^3/d.

CRediT authorship contribution statement

Xiu-Chao Jiang: Writing – original draft, Investigation. **Xiao-Hu Dong:** Writing – review & editing, Supervision, Methodology. **Hao Zhang:** Investigation, Formal analysis. **Tian-Yang Yin:** Investigation. **Hui-Qing Liu:** Supervision, Resources.

Declaration of competing interest

The authors declare that they have no known competing financial interests or personal relationships that could have appeared to influence the work reported in this paper.

Acknowledgments

This work was financially supported by the National Key R&D Program of China (Grant No. 2024YFF0508900).

Nomenclature

g	Acceleration due to gravity, m/s^2
h_m	Experimental pay zone thickness, m
h_p	Field-scale pay zone thickness, m
i	Oil layer number
i_s	Steam injection rate (cold water equivalent), m^3/s
K	Reservoir permeability, 10^{-3} μm^2
L	Well spacing, m
L_m	Experimental well spacing, m
L_p	Field-scale well spacing, m
m	Count of oil layers
N	Reserve under well control, m^3
q_i	Steam injection or oil production rate, mL/min
q_d^i	Dimensionless steam injection or oil production ratio
Q_s	Cyclic steam injection volume (cold water equivalent), m^3
t	Production time, s
t_s	Injection time, s
V	Reservoir bulk volume, m^3
V_r	Variation coefficient of the heated chamber proportion
α	Thermal diffusivity, m^2/s
α_{avg}	Average proportion of the heated chamber
α_i	Proportion of the heated chamber of the ith oil layer
ΔS_o	Movable oil saturation
μ_o	Oil viscosity, mPa·s
ρ_o	Oil density, kg/m^3
ϕ	Porosity

References

Araújo, E.A., Batista, L.C., Bechara, J.V.O., Gurgel, A.R., Oliveira, G.P., Aum, P.T.P., 2022. Influence of high permeability subdomains on steam injection performance in heavy-oil reservoirs. J. Petrol. Sci. Eng. 208, 109388. https://doi.org/10.1016/j.petrol.2021.109388.

Austin-Adigio, M., Gates, I., 2019. Non-condensable gas co-injection with steam for oil sands recovery. Energy 179, 736–746. https://doi.org/10.1016/j.energy.2019.05.034.

Cai, H., Zou, J., 2024. Technical challenges, current situation, and prospects of thermal recovery of heavy oil in Bohai oilfield. China Offshore Oil Gas 36 (5), 157–169. https://doi.org/10.11935/j.issn.1673-1506.2024.05.016 (in Chinese).

Chai, M., Chai, L., Nourozieh, H., Chen, Z., Yang, M., 2024. A technical, economic, and environmental assessment on dimethyl ether (DME) as a renewable solvent from carbon dioxide utilization (CCU) for heavy oil recovery: A real field in Surmont, Canada as case study. Chem. Eng. J. 482, 148936. https://doi.org/10.1016/j.cej.2024.148936.

Chen, Q., Ye, M., Wang, D., Wang, Y., Wang, Z., Pu, W., Wei, B., 2024. Active polymer flooding for strongly heterogeneous reservoir associate with foam combination technology. Geoenergy Sci. Eng. 242, 213288. https://doi.org/10.1016/j.geoen.2024.213288.

Dang, F., Li, S., Feng, S., 2025. Greening strategy for heavy oil thermal recovery assisted by environmental-friendly solvent dimethyl ether. Geoenergy Sci. Eng. 251, 213889. https://doi.org/10.1016/j.geoen.2025.213889.

Ding, B., Dong, M., Chen, Z., Kantzas, A., 2022. Enhanced oil recovery by emulsion injection in heterogeneous heavy oil reservoirs: Experiments, modeling and reservoir simulation. J. Petrol. Sci. Eng. 209, 109882. https://doi.org/10.1016/j.petrol.2021.109882.

Dong, Q., 2018. Annual adjustable layered steam injection and its application. Special Oil Gas Reservoirs 25 (5), 168–171. https://doi.org/10.3969/j.issn.1006-6535.2018.05.032 (in Chinese).

Dong, X., Liu, H., Chen, Z., Wu, K., Lu, N., Zhang, Q., 2019. Enhanced oil recovery techniques for heavy oil and oilsands reservoirs after steam injection. Appl. Energy 239, 1190–1211. https://doi.org/10.1016/j.apenergy.2019.01.244.

Dong, X., Jiang, X., Zheng, W., Liu, H., Liu, R., Wang, W., Zeng, D., Wang, T., 2022. Discussion on the sweep efficiency of hybrid steam–chemical process in heavy oil reservoirs: An experimental study. Pet. Sci. 19 (6), 2905–2921. https://doi.org/10.1016/j.petsci.2022.06.018.

Dong, X., Liu, H., Tian, Y., Liu, S., Li, J., Jiang, L., Chen, Z., 2024. A new method to reduce shale barrier effect on SAGD process: Experimental and numerical simulation studies using laboratory-scale model. SPE J. 29 (4), 2044–2059. https://doi.org/10.2118/218390-PA.

Gao, H., Pu, W., Li, Y., Luo, Q., Sun, Z., 2020. Deep profile control experiment of in-situ gel after steam flooding in heavy oil reservoir. Reservoir Eval. Dev. 10 (6), 58–64. https://doi.org/10.13809/j.cnki.cn32-1825/te.2020.06.009 (in Chinese).

Gong, Y., Wang, Z., Zhao, C., Gong, Y., Li, Y., 2007. Convert to steam flooding after cyclic steam stimulation in Block Qi40. Special Oil Gas Reservoirs 14 (6), 17–21 (in Chinese).

Guan, W., Jiang, Y., Guo, E., Wang, B., 2023. Heavy oil development strategy under the "Carbon Peaking and Carbon Neutrality" target. Acta Pet. Sin. 44 (5), 826–840. https://doi.org/10.7623/syxb202305008 (in Chinese).

He, W., Sun, X., Wu, Y., Luo, C., Guo, H., Zhang, J., Li, S., 2024. Optimization design and field test of SAGD electric heating preheating start-up parameters for double horizontal wells in shallow super-heavy oil reservoirs. Special Oil Gas Reservoirs 31 (6), 77–83. https://doi.org/10.3969/j.issn.1006-6535.2024.06.009 (in Chinese).

Hong, Q., Pang, Z., Liu, X., Wang, B., Liu, D., Liao, H., Wang, L., 2025. Quantitative macro and micro analysis on enhanced oil recovery (EOR) mechanisms of multi-component composite steam flooding (MCCSF) based on image recognition algorithm. Geoenergy Sci. Eng. 249, 213766. https://doi.org/10.1016/j.geoen.2025.213766.

Hoyos Perdomo, R., Ardila Cubillos, L.J., Munoz Navarro, S.F., Rincon Canas, M.M., Palma-Bustamante, J.M., Naranjo Suarez, C.E., 2014. Evaluation of different strategies for selective steam injection in stratified heavy-oil reservoirs. In: SPE Latin America and Caribbean Heavy and Extra Heavy Oil Conference. https://doi.org/10.2118/171143-MS.

Huang, S., Kang, B., Cheng, L., Zhou, W., Chang, S., 2015. Quantitative characterization of interlayer interference and productivity prediction of directional wells in the multilayer commingled production of ordinary offshore heavy oil reservoirs. Petrol. Explor. Dev. 42 (4), 533–540. https://doi.org/10.1016/S1876-3804(15)30046-X.

Huang, S., Chen, X., Liu, H., Xia, Y., Jiang, J., Cao, M., Li, A., Yang, M., 2019. Experimental and numerical study of steam-chamber evolution during solvent-enhanced steam flooding in thin heavy-oil reservoirs. J. Petrol. Sci. Eng. 172, 776–786. https://doi.org/10.1016/j.petrol.2018.08.071.

Jamshid-nezhad, M., 2022. Steam alternating non-condensable gas injection for more heavy oil recovery. Energy 240, 122476. https://doi.org/10.1016/j.energy.2021.122476.

Jiang, X., Dong, X., Xu, W., Liu, H., Chen, Z., 2024. Mathematical modeling for the production performance of cyclic multi-thermal fluid stimulation process in layered heavy oil reservoirs. Geoenergy Sci. Eng. 243, 213350. https://doi.org/10.1016/j.geoen.2024.213350.

Kang, B., Jiang, B., Chen, G., Li, C., Gao, Y., 2021. Research and application of interlayer interference law in multi-layer bottom water reservoir: Taking QHD32-6 as an example. J. Chongqing Univ. Sci. Technol. (Nat. Sci. Ed.) 23 (4), 18–23. https://doi.org/10.19406/j.cnki.cqkjxyxbzkb.2021.04.004 (in Chinese).

Li, B., Tao, L., Zhang, N., Wang, K., Li, Z., 2019. The influence of surfactants on the flow characterization of heavy oil. Petrol. Sci. Technol. 37 (2), 155–162. https://doi.org/10.1080/10916466.2018.1522337.

Li, B., Li, B., Sun, X., Zhu, D., Chen, S., Li, Z., Tao, L., Zhang, J., 2025a. Enhanced recovery in heavy oil reservoirs with interlayers using flue gas-assisted VH-SAGD: A 2D visualization study. Pet. Sci. 22 (8), 3418–3433. https://doi.org/10.1016/j.petsci.2025.05.007.

Li, S., Peng, D., Feng, S., Wang, Z., Zhang, K., 2023a. Dimethyl ether-steam assisted gravity drainage: Physical 2D heavy oil simulation. Fuel 342, 127821. https://doi.org/10.1016/j.fuel.2023.127821.

Li, S., Wang, C., Wu, Y., Liu, P., Zhang, X., Liu, P., Xi, C., Wang, Q., Zhang, J., 2025b. Experimental and numerical simulation studies on sweep efficiency in electrical heating-CO_2 assisted SAGD for heavy oil reservoirs with interbeds. Geoenergy Sci. Eng. 252, 213941. https://doi.org/10.1016/j.geoen.2025.213941.

Li, X., Sun, X., Cai, J., Zhang, Q., Pan, X., Zhang, Y., 2023b. Experimental investigation on supercritical multi-thermal fluid flooding using a novel 2-dimensional model. Energy 283, 129136. https://doi.org/10.1016/j.energy.2023.129136.

Liu, H., Dong, X., 2022. Current status and future trends of hybrid thermal EOR processes in heavy oil reservoirs. Petrol. Sci. Bull. 7 (2), 174–184. https://doi.org/10.3969/j.issn.2096-1693.2022.02.015 (in Chinese).

Liu, H., Wang, Z., Huang, C., Liu, R., Li, Y., Su, Y., 2007. Research and application of separate layer steam injection technology. Petrol. Geol. Eng. 21 (3), 79–81 (in Chinese).

Liu, Q., 2022. Study and test on steam flooding technology for thin interbedded ultra-heavy oil reservoirs. Special Oil Gas Reservoirs 29 (6), 97–103. https://doi.org/10.3969/j.issn.1006-6535.2022.06.012 (in Chinese).

Liu, W., 2013. Analysis on production performance and research on influencing factors of sweep efficiency of steam flooding in Block Qi40. Ph.D Dissertation. Northeast Petrol. Univ. (in Chinese).

Liu, W., Du, L., Zou, X., Liu, T., Wu, X., Wang, Y., Dong, J., 2023. Experimental study on the enhanced ultra-heavy oil recovery using an oil-soluble viscosity reducer and CO_2 assisted steam flooding. Geoenergy Sci. Eng. 222, 211409. https://doi.org/10.1016/j.geoen.2022.211409.

Lu, N., Dong, X., Liu, H., Chen, Z., Xu, W., Zeng, D., 2024. Molecular insights into the synergistic mechanisms of hybrid CO_2-surfactant thermal systems at heavy oil-water interfaces. Energy 286, 129476. https://doi.org/10.1016/j.energy.2023.129476.

Pang, Z., Wang, Q., Meng, Q., Wang, B., Liu, D., 2024. The mechanisms of thermal solidification agent promoting steam diversion in heavy oil reservoirs. Pet. Sci. 21 (3), 1902–1914. https://doi.org/10.1016/j.petsci.2024.01.001.

Peng, Y., Zhang, Y., Zhang, M., Ju, B., Pang, C., Xu, D., 2025. Analytical solution of oil and water two-phase Buckley-Leverett equation in inclined stratified heterogeneous reservoirs. Geoenergy Sci. Eng. 251, 213849. https://doi.org/10.1016/j.geoen.2025.213849.

Pérez, R.A., García, H.A., Gutiérrez, D., Rodríguez, H.A., Mehta, S., Moore, R.G., Ursenbach, M., Sequera-Dalton, B., Manrique, E.J., 2022. Energy efficient steam-based hybrid technologies: Modeling approach of laboratory experiments. In: SPE Improved Oil Recovery Conference. https://doi.org/10.2118/209439-MS.

Pratama, R.A., Babadagli, T., 2024. What is next for SAGD? Evaluation of low GHG and high-efficiency tertiary recovery. Geoenergy Sci. Eng. 234, 212608. https://doi.org/10.1016/j.geoen.2023.212608.

Pu, B., Cao, R., Yan, G., Yu, J., Jia, Z., Cheng, L., Sun, Y., 2025. Pore network modeling of quasi-static two-phase flow considering modification of pore-scale remaining oil saturation during high-flux water flooding. SPE J. 30 (5), 2923–2941. https://doi.org/10.2118/225413-PA.

Ren, F., Sun, H., Hu, C., 2012. Heavy oil development technology and practices in Liaohe Oilfield. Special Oil Gas Reservoirs 19 (1), 1–8 (in Chinese).

Rui, Z., Liu, T., Wen, X., Meng, S., Li, Y., Dindoruk, B., 2025. Investigating the synergistic impact of CCUS-EOR. Eng. 48, 16–40. https://doi.org/10.1016/j.eng.2025.04.005.

Shan, C., 2023. Study on Oil Temperature Optimization of Crude Oil Handover in an Oil Field. Master's Thesis. China University of Petroleum (East China) https://doi.org/10.27643/d.cnki.gsybu.2023.001140. (in Chinese)

Shen, D., Wu, Y., Liang, S., Luo, J., 2015. Thermal stability of foam during steam drive. Petrol. Explor. Dev. 42 (5), 712–716. https://doi.org/10.1016/S1876-3804(15)30067-7.

Shen, X., Liu, H., Zhang, Y., Xu, H., Fan, X., Ma, L., Shang, X., 2022. Identification method for high water consumption layer in second oil recovery based on machine learning. Drill. Prod. Technol. 45 (4), 74–80 (in Chinese).

Sheng, X., Lin, S., Liang, W., Xie, H., Liu, M., 2025. Optimal long-term planning of CCUS and carbon trading mechanism in offshore-onshore integrated energy system. Appl. Energy 379, 124983. https://doi.org/10.1016/j.apenergy.2024.124983.

Song, X., Li, Y., Li, F., Yi, L., Song, B., Zhu, G., Su, H., Wei, L., Yang, C., 2024. Separate-layer balanced waterflooding development technology for thick and complex carbonate reservoirs in the Middle East. Petrol. Explor. Dev. 51 (3), 661–673. https://doi.org/10.1016/S1876-3804(24)60495-7.

Sun, H., Liu, H., Wang, H., Shu, Q., Wu, G., Yang, Y., 2022. Development technology and direction of thermal recovery of heavy oil in China. Acta Pet. Sin. 43 (11), 1664–1674 (in Chinese).

Sun, H., Yang, Y., Wang, H., Wang, J., Wu, G., Cui, Y., Yu, Q., 2023a. Distribution characteristics of remaining oil in extra-high water cut reservoirs and new

technologies for enhancing oil recovery. J. China Univ. Petrol. (Ed. Nat. Sci.) 47 (5), 90–102. https://doi.org/10.3969/j.issn.1673-5005.2023.05.009 (in Chinese).
Sun, Q., 2020. Study on Integrated Technology of Stratified Sand Control and Steam Injection in Shanjiasi Reservoir. Master's Thesis. China University of Petroleum (East China). https://doi.org/10.27644/d.cnki.gsydu.2020.001137 (in Chinese).
Sun, X., Wei, C., Zhang, Q., Cai, J., Wang, X., Wang, Y., Zhang, Y., 2023b. Development of a generalized experimental methodology for investigating the role of steam quality on steamflooding performance. SPE J. 28 (1), 401–414. https://doi.org/10.2118/210595-PA.
Tang, H., Zhang, K., Tang, R., Lyu, D., Tan, L., 2022. The essence and re-recognition of interlayer interference. J. Southwest Petrol. Univ. (Sci. Technol. Ed.) 44 (5), 113–124. https://doi.org/10.11885/j.issn.1674-5086.2022.04.12.03 (in Chinese).
Venkat Venkatramani, A., Okuno, R., 2017. Characterization of reservoir heterogeneity for SAGD and ES-SAGD: Under what type of heterogeneity is ES-SAGD more likely to lower SOR?. In: SPE Annual Technical Conference and Exhibition https://doi.org/10.2118/187427-MS.
Wang, K., Wang, Y., Yang, Y., Liu, X., 2018. A new method to calculate the injection quantity of stratified gas injection in normal heavy oil reservoirs. Petrol. Geol. Eng. 32 (5), 91–94 (in Chinese).
Wang, L., Liu, T., Cai, Y., 2017. Optimization of successive development methods of inclined reservoirs at late stage of steam flooding: A case study from Block Qi 40 in western sag of Liaohe rifted basin. Xinjing Pet. Geol. 38 (3), 319–324 (in Chinese).
Wang, S., Shi, L., Ye, Z., Wang, Y., Liu, C., Xue, X., 2021. Microscopic experimental study on the sweep and displacement efficiencies in heterogeneous heavy oil reservoirs. Energy Rep. 7, 1627–1635. https://doi.org/10.1016/j.egyr.2021.03.018.
Wang, Y., 2021. Study on the Water Invasion Law with Thermal Production and Chemical Cold Recovery Mechanisms in Heavy Oil Reservoirs with Edge Water. Ph.D Dissertation. China University of Petroleum (Beijing). https://doi.org/10.27643/d.cnki.gsybu.2021.000159 (in Chinese).
Wang, Y., Liu, H., Zhang, Q., Chen, Z., Wang, J., Dong, X., Chen, F., 2020. Pore-scale experimental study on EOR mechanisms of combining thermal and chemical flooding in heavy oil reservoirs. J. Petrol. Sci. Eng. 185, 106649. https://doi.org/10.1016/j.petrol.2019.106649.
Wang, Z., Li, S., Li, Z., 2022. A novel strategy to reduce carbon emissions of heavy oil thermal recovery: condensation heat transfer performance of flue gas-assisted steam flooding. Appl. Therm. Eng. 205, 118076. https://doi.org/10.1016/j.applthermaleng.2022.118076.
Wang, Z., Du, H., Li, S., Li, S., 2023. Experimental study on gas-assisted cyclic steam stimulation under heavy-oil sandstone reservoir conditions: Effect of N_2/CO_2 ratio and foaming agent. Geoenergy Sci. Eng. 228, 211976. https://doi.org/10.1016/j.geoen.2023.211976.
Wang, Z., Liu, H., Sun, Z., Wang, Y., Luo, C., Pan, Y., 2024. Study on characterization of interlayer heterogeneity in commingling production reservoirs. Petrol. Geol. Recov. Effic. 31 (3), 42–53. https://doi.org/10.13673/j.pgre.202304011 (in Chinese).
Wu, Z., Pang, Z., Liu, H., Wang, D., Wang, C., Wang, C., Ye, Z., Chen, Y., 2015. A visible experiment on adoption of high-temperature gel for improving the development effect of steam flooding in heavy oil reservoirs. Acta Pet. Sin. 36 (11), 1421–1426. https://doi.org/10.7623/syxb201511011 (in Chinese).
Wu, Z., Liu, H., Wang, X., Zhang, Z., 2018. Emulsification and improved oil recovery with viscosity reducer during steam injection process for heavy oil. J. Ind. Eng. Chem. 61, 348–355. https://doi.org/10.1016/j.jiec.2017.12.033.
Xiong, Y., Hao, D., Zhang, L., Wang, F., Song, C., Li, Y., 2016. Test and effect evaluation of stratified steam injection technology for heavy oil in Fuyu oilfield—Take the Block91 as an example. Unconv. Oil Gas 3 (6), 72–76 (in Chinese).
Yan, X., Pang, Z., Liu, D., Wang, B., 2025. The characteristics of steam chamber expanding and the EOR mechanisms of tridimensional steam flooding (TSF) in thick heavy oil reservoirs. Geoenergy Sci. Eng. 244, 213434. https://doi.org/10.1016/j.geoen.2024.213434.
Yang, L., Yuan, A., Long, H., Zhang, F., Wu, X., Yang, X., Yang, X., Liu, F., Li, C., 2024a. Research and experiment on electrification technology for deep heavy oil reservoir. In: Abu Dhabi International Petroleum Exhibition and Conference. https://doi.org/10.2118/221917-MS.
Yang, S., Huang, S., Jiang, Q., Jiang, G., Liu, Q., Wang, Z., Gong, R., 2024b. In-situ solvents generation enhanced steam assisted gravity drainage (ISSG-SAGD): A low carbon and high-efficiency approach for heavy oil recovery. Energy 291, 130370. https://doi.org/10.1016/j.energy.2024.130370.
Zhang, W., Zhou, F., Lin, S., Wang, H., Wang, Q., Zhang, J., Wang, X., Dong, Q., 2025. Zone division and injection method in soaking condition of offshore heavy oil reservoir. J. China Univ. Petrol. (Ed. Nat. Sci.) 49 (2), 231–239. https://doi.org/10.3969/j.issn.1673-5005.2025.02.023 (in Chinese).
Zhao, D., Hou, J., Sun, J., Shi, L., Du, Q., Li, J., 2022. Interwell connectivity inversion method of steam flooding: Based on an analytical model and genetic algorithm. J. Petrol. Sci. Eng. 215, 110641. https://doi.org/10.1016/j.petrol.2022.110641.
Zhao, H., 2009. Study and application of heavy oil steam flooding in mid-deeplayers in Liaohe oilfield. Oil Drilling & Production Technology 31 (S1), 110–114 (in Chinese).
Zhao, W., Wang, J., Qian, Q., Yu, C., Zhang, M., Liu, H., Huang, Y., 2023. Evolution law of dominant flow channels of water flooding in heterogeneous reservoir. Fault-Block Oil Gas Field 30 (5), 847–857 (in Chinese).
Zhu, D., Li, B., Li, B., Husein, M.M., Xu, Z., Wang, H., Li, Z., 2024. Experimental study of viscosity reducer-assisted gas huff-n-puff in heavy oil reservoirs. Geoenergy Sci. Eng. 243, 213399. https://doi.org/10.1016/j.geoen.2024.213399.
Zhu, Q., Jia, X., Li, B., Wang, K., Zhang, Y., Chen, Z., 2022. Mathematical modeling of foamy-oil flow in a cyclic solvent injection process. J. Petrol. Sci. Eng. 215, 110594. https://doi.org/10.1016/j.petrol.2022.110594.